



**HAL**  
open science

## Unravelling the consequences of ultra-fine milling on physical and chemical characteristics of flax fibres

Claire Mayer-Laigle, Alain Bourmaud, Darshil U. Shah, Nadège Follain,  
Johnny J. Beaugrand

► **To cite this version:**

Claire Mayer-Laigle, Alain Bourmaud, Darshil U. Shah, Nadège Follain, Johnny J. Beaugrand. Unravelling the consequences of ultra-fine milling on physical and chemical characteristics of flax fibres. Powder Technology, 2020, 360, pp.129-140. 10.1016/j.powtec.2019.10.024 . hal-02342154

**HAL Id: hal-02342154**

**<https://hal.science/hal-02342154>**

Submitted on 21 Dec 2021

**HAL** is a multi-disciplinary open access archive for the deposit and dissemination of scientific research documents, whether they are published or not. The documents may come from teaching and research institutions in France or abroad, or from public or private research centers.

L'archive ouverte pluridisciplinaire **HAL**, est destinée au dépôt et à la diffusion de documents scientifiques de niveau recherche, publiés ou non, émanant des établissements d'enseignement et de recherche français ou étrangers, des laboratoires publics ou privés.



Distributed under a Creative Commons Attribution - NonCommercial 4.0 International License

## Unravelling the consequences of ultra-fine milling on physical and chemical characteristics of flax fibres

Claire Mayer-Laigle<sup>1</sup>, Alain Bourmaud<sup>2</sup>, Darshil U. Shah<sup>3</sup>, Nadège Follain<sup>4</sup>, Johnny Beaugrand<sup>5</sup>

<sup>(1)</sup> IATE, Univ Montpellier, CIRAD, INRA, Montpellier SupAgro, Montpellier, France

<sup>(2)</sup> Univ. Bretagne Sud, UMR CNRS 6027, IRDL, F-56100 Lorient, France

<sup>(3)</sup> Centre for Natural Material Innovation, Dept. of Architecture, University of Cambridge, Cambridge CB2 1PX, UK

<sup>(4)</sup> Normandie Univ, UNIROUEN Normandie, INSA Rouen, CNRS, PBS, 76000 Rouen, France

<sup>(5)</sup> Biopolymères Interactions Assemblages (BIA), INRA, Nantes, France

**Corresponding author:** Claire Mayer-Laigle; +33 499 612 563; [claire.mayer@inra.fr](mailto:claire.mayer@inra.fr)

### **Abstract :**

In recent years, lignocellulosic biomass has been increasingly used in various applications. While for many of them the plant materials require coarse milling, some new applications for green chemistry, bio-energy and bio-packaging necessitate comminution to obtain very finely calibrated particles (below 200  $\mu\text{m}$  in size). This milling step is not inconsequential for lignocellulosic materials and can influence the physical and chemical characteristics of the powder. However, these different effects are still poorly understood. In this work, we study the impact of ultra-fine milling on the physico-chemical properties of plant fibres. Flax was chosen for this study because of its **well-described** structure and biochemical **composition**, making it a model material. Our main results evidence a strong impact of ball milling on flax fibre aspect ratio but also on cell wall ultrastructure and composition. Cellulose content and crystallinity significantly decrease with milling time, leading to higher water sorption and lower thermal stability.

**Keywords:** ball milling ; milling kinetics; lignocellulosic biomass; particle shape; cellulose content; crystallinity

### **1. Introduction**

In material processing, the aim of a grinder is to generate a fracture path which will propagate through the material and lead to its rupture. Depending on the technology selected, as well as the process parameters and the mechanical properties of the raw materials, the energy consumption of the operation can significantly differ and the ground product can exhibit various properties, including shape, specific surface area, and flow behaviour. This has been demonstrated in numerous studies on inorganic powders [1-6]. In contrast, the milling – especially ultra-fine milling – of plant materials is still poorly explored [7]. New technical applications increasingly require the use of ever finer plant cell wall powders. In particular, applications such as gasification processes [8], direct combustion in engine [9], filler for packaging [10], green chemistry [11, 12], and 3D printing of renewable biobased powder [13] require drastic reduction in particle size to below 200 microns. Nevertheless, due to the inherently large heterogeneity in plant materials, it can be difficult to obtain uniformity.

Lignocellulosic biomass is mainly composed of three macromolecules – cellulose, hemicellulose and lignin – alongside organic extractable compounds, which are generally mixtures of low molecular weight molecules, soluble proteins, non-cellulosic saccharides and phenolic components, as well as mineral inclusions, such as silica deposits in e.g. rice husks [14] and date palm fibres [15]. The three macromolecules are bonded together in a complex way through different types of bonds, mainly ester, ether, carbon-carbon or hydrogen bonds [16]. The relative proportion of each constituent of the lignocellulosic biomass varies considerably with the taxonomic group, plant species, genetic variety, geographic area and growing conditions of the fibre crop [17]. In addition to this chemical heterogeneity, lignocellulosic biomass exhibit structural and physical heterogeneity at different scales [7]. At the macroscopic scale, the organization of the different polymers that support the stalk during plant growth result in a fibrous material with an anisotropic structure: mechanical properties (Young's modulus, tensile strength, Poisson ratio, etc.) are different in the longitudinal and transverse directions [18]. These properties are partly related to the chemical composition, in particular to the ultrastructural organization of the cellulose fibril inside the plant materials, but also to lignin content [19]. At the histological scale, tissues may have similar composition or architecture which in turn influences mechanical properties, as observed in sorgo or miscanthus stems [20, 21]. These plant materials have an aerated inner section, known as pith, which is mainly composed of parenchyma and vascular

bundles, and an outer section, the ring, which is made of epidermis, parenchyma and vascular bundles. The inner part is a solid highly compressible foam with useful noise and thermal insulating properties, whereas the outer part is dense and more rigid [22].

Much research regarding the milling of plant materials is related to coarse milling with a focus on the shape of the ground powder and on energy consumption during processing [18, 23-25]. Coarse milling can be assimilated with homothetic comminution where plant tissues maintain structural coherency at the particle scale. In contrast, intense comminution leads to cellular scale effects (ca. 50  $\mu\text{m}$ ) and generates particles that exhibit different size, shape, and compositional properties provoking the release of cellular constituents. The influence of such intense ultra-fine milling on the physical and chemical properties of the ground powder have not yet been fully explored. Karinkanta et al. [26] have shown for wood powder that the milling technology chosen affects the size of the resulting particle, their aspect ratio and **energy consumption during the milling step**. Intense milling can also significantly decrease the crystallinity of cellulose. This point has been raised by several authors studying pure crystalline cellulose [27-29] and has also been confirmed on wood and straw powder by Schwanninger et al. [30] and Silva et al. [31], respectively. However, such amorphization is dependent on the milling technology employed and is more pronounced for ball-milling than jet-milling, probably due to mechanical effects of the repeated impacts of balls on cellulose chain **in the case of the former** [31, 32]. Modification of water-holding capacity (WHC) of plant material in relation to milling technique has also been reported, however, findings are contradictory. In some cases, an increase in WHC is observed and attributed to the increase in specific surface area, which leads to the exposure of more hydrophilic groups belonging to cellulose and hemicelluloses [33, 34]. However, Raghavendra et al [35] have observed inverse trends during the milling of coconut residues and explain it by the amorphization of the cellulose together with a reduction of porosity.

Thus, due to its complex and heterogeneous structure at different scales, the behaviour of the plant materials during milling is difficult to predict and the properties of the ground powder are not generalizable. Further exploratory work is needed on model plant materials to improve our knowledge of the impact of grinding, and especially the ultra-fine grinding stage on the properties of the ground powder while unravelling the effects of grinding from those due to biomass variability.

Among the great diversity of plant materials, flax fibres can be viewed as model cellulosic materials [36]. A single flax fibre is composed of a thin primary wall which surrounds a thick secondary wall, reinforced by cellulose microfibrils, and a central cavity, named lumen [37]. Microfibrils are coated with hemicelluloses and embedded in a matrix of incrusting pectins [38-40], they are oriented at an angle of around 10° in relation to the fibre axis. The secondary wall represents 80% of the cross-section of fibres, and is mainly responsible for the fibre's mechanical properties, giving them a high potential as composite reinforcements. Flax fibres have a high cellulose content (close to 80%) which varies slightly with plant variety [41], agronomic practice [42, 43], growth conditions [44] and maturity [45]. Nonetheless, these variations remain significantly lower in comparison to other lignocellulosic biomasses.

In this work, we explored the effects of the milling step on the physical and chemical characteristics of flax fibres. Flax was selected as a model plant material due to its hierarchical structure, its high cellulose content and also relatively little scatter in properties. Initially, different grinding technologies were explored on mm-scale flax fibres in order to select an appropriate grinding process allowing efficient conversion of the raw materials into ultrafine particles. Then, for the most promising grinding technique, a range of grinding time periods were studied. The morphology of the flax particles obtained was then explored by morphological analysis and electron microscopy. In addition, we report and discuss the impact of grinding time on flax biochemical composition, water hygroscopic capacity, crystallinity and thermal behaviour.

## **2. Material and Methods :**

### **2.1 Raw materials**

Flax (*Linum usitatissimum* L.) fibres from the Alizé variety were selected for this work. The flax plant was cultivated in Normandy and harvested at the end of June 2015 when the seeds were mature. The plants were then laid on the soil to enable dew-retting. After the harvest, the plants were stored, scutched and the fibres were classified by farmers using an organoleptic system of notation which takes into account the handling, toughness, colour, strength, fineness and homogeneity. The fibres were then hackled and cut into 1 mm lengths on average.

## 2.2 Milling processes

In order to produce fine flax powders, several grinding technologies generating different mechanical stresses were explored. First an impact mill (UPZ 100, Howokawa Alpine<sup>®</sup>) equipped with a screen of 0.3 mm and 0.1 mm were used to produce samples named FLAX 1 and FLAX 2, respectively. The feed rate was 0.5 kg.h<sup>-1</sup> and rotor speed was set at 18,000 rpm. Then the FLAX 1 and FLAX 2 were ground a second time on a centrifugal mill (ZM200, Retsch<sup>®</sup>) equipped with a screen of 0.12 mm to obtain the samples named FLAX 3 and FLAX 4. The rotor speed was set at 22,000 rpm. To control the strong rise in temperature during milling, the mill was fed manually, at a rate of approximately 0.1 kg. h<sup>-1</sup>. In parallel, the raw flax fibres were also milled in a vibratory Ball Mill (DM1, Sweco<sup>®</sup>). The device is a batch grinder. A grinding chamber of 36 L in abrasion-resistant elastomer is filled with 25 kg of ceramics cylinders (diameter and length: 13.5 mm) and 25 kg of ceramics balls (diameter 13.5 mm). The chamber is put in motion by a vibrating mechanism composed of high-tensile steel springs. The amplitude of the vibrations is a function of the whole charge of the chamber and the stiffness of the spring. Here, 1 kg of flax fibre was first dried in an oven at 60 °C for 24 hours, and then introduced into the milling chamber. Samples were withdrawn after different milling times (1H00, 2H20, 5H30, 7H00, 8H00, 10H00, 17H00, 23H00) to monitor the evolution of the powder properties during the grinding process. The different samples were named FLAX BM followed by the milling time. The energy consumption (J) during milling was determined by multiplying the milling time (in second) by the power consumed (W or J·s<sup>-1</sup>) in operation measured with a wattmeter Meteix PX 120 on the electric grid.

## 2.3 Measurement of particle size

The evolution of particle size distribution of the ground flax particles was monitored using a laser diffraction particle size analyzer Hydro 2000S (Malvern Instruments Ltd., United Kingdom), with liquid ethanol (ethylic alcohol: 96% v/v) as carrier. From the diffraction image, the particle sizes were determined using the Mie method with a refraction index of 1.53 [46]. The results were expressed in volume based on the assumption that the particles were spherical. Measurements were made in triplicate and the median particle size (d50), the 10<sup>th</sup> percentile (d10) and the 90<sup>th</sup> percentile (d90) were then calculated. From the

particle size distribution, the specific surface area, which corresponds to the total surface developed by the powder, was also determined according to the following equation from this particle size distribution; the specific surface per unit of mass denoted  $S$  (in  $\text{kg.m}^{-2}$ ) was evaluated according to the following equation :

$$S = \frac{1}{\rho} \sum_i \frac{3\alpha_i}{R_i} \quad (\text{Eq. 1})$$

where  $\rho$  is the true density of powder,  $i$  the index grading class (between  $0.02$  and  $2000\mu\text{m}$ ),  $\alpha_i$  is the volume fraction and  $R_i$  the average radius of particles in the  $i^{\text{th}}$  class.

#### 2.4 Measurement of particle shape

**Scanning electron microscope (SEM) observation:** For ground powders FLAX 1-4, SEM observations were performed with a scanning electron microscope Phenom Pro-X (Phenom, France) using a charge reduction sample holder under a voltage of  $10$  kV. For ground powders FLAX BM 1H00-23H00, SEM observation were performed with a JEOL JSM 6460LV (Jeol, Croissy Sur Seine, France) SEM. In this case, the powders were first sputter coated with gold prior to the observation;  $20$  kV voltage was used.

**Quantitative morphological analysis:** The lengths ( $L$ ) and diameters ( $D$ ) of the ground particles were obtained with a MorFi Compact<sup>®</sup> fibre analyzer (Techpap SAS, Grenoble, France). The analysis was performed in dynamic mode via the measurement of flax suspension (of approximately  $50$  mg/L) in distilled water flowing through the recording cell. A camera with a resolution of  $1280 * 960$  pixels and an accuracy of approximately  $10\mu\text{m}/\text{pixel}$  [47] recorded the fibres' images. Analyses were performed in triplicate and the mean values were determined. A minimum of thousand elements were counted for each composition, in order to provide a statistically valid sample population.

#### 2.5 Thermogravimetric analysis

Experiments were performed using a Setaram<sup>TM</sup> 92 apparatus. The heating rate was  $10^\circ\text{C.min}^{-1}$  under air atmosphere from  $25^\circ\text{C}$  to  $900^\circ\text{C}$ . Around  $40$  mg of each kind of fibre was used. Weight change versus temperature was recorded.

#### 2.6 Monosaccharide content

The monosaccharide content of raw flax fibre and the ground flax powders at different strategic milling time were determined by chemical analysis. The size of the raw flax requires a first step of homogenization. This was done by cryogrinding approximately 3g of raw flax fibre into a fine powder on a centrifugal mill ZM100 (Retsch®, France) equipped with a 0.1 mm sieve. RAW FLAX and FLAX BM samples (Fig 1) were then subjected to hydrolysis in 12 M H<sub>2</sub>SO<sub>4</sub> for 2 h at 25°C (heat plate) followed by additional hydrolysis of 2 h at 100°C with 1.5 M H<sub>2</sub>SO<sub>4</sub> in presence of inositol as internal standard. Galacturonic Acid (GalA) was determined by an automated m-hydroxybiphenyl method [48] whereas individual neutral sugars (arabinose, fucose, glucose, xylose, galactose and mannose) were analyzed as their alditol acetate derivatives [49] by gas-liquid chromatography (Perkin Elmer, Clarus 580, Shelton, CT, USA) equipped with an DB 225 capillary column (J&W Scientific, Folsom, CA, USA) at 205 °C, with H<sub>2</sub> as the carrier gas. Standard sugar solutions were used for calibration. Analyses were performed in three independent assays. The total monosaccharide content is the sum of each monosaccharide amounts, and is expressed as the percentage of the dry matter mass. All the chemicals were laboratory grade, obtained from Sigma Aldrich.

### 2.7 Measurement of cellulose crystallinity

The cellulose crystallinity was determined by wide-angle X-ray diffraction (WAXRD) measurements performed under ambient conditions on a Siemens D500 diffractometer CuK $\alpha$  radiation. Samples were loaded on a silicon wafer and scans were collected from 2 $\theta$  = 10 to 40° with step size of 0.03° at 2 s/step, at 30 kV and 20 mA. Crystallinity was calculated using Eq. 2,

$$C = \frac{I_{tot} - I_{am}}{I_{tot}} * 100 \quad (\text{Eq. 2})$$

Where  $I_{tot}$  is the intensity at the primary peak for cellulose I (at 2 $\theta$   $\approx$  22.5°) and  $I_{am}$  is the intensity from the amorphous phase evaluated as the minimum intensity (at 2 $\theta$   $\approx$  18.5°) [50]

### 2.8 Dynamic Vapour sorption measurement

The water vapour sorption measurements were carried out at 25°C using an automatic Dynamic Vapour Sorption analyzer (Surface Measurement Systems LTD., U.K.) equipped with an electronic microbalance (Cahn D200) having a 0.1  $\mu$ g mass resolution. After conducting a

dehydration step and measuring the initial mass, approximately 16 mg of each flax sample was submitted to a hydration cycle with water vapour activities,  $a$ , varying from 0 to 0.95 in order to collect the kinetic data, i.e. mass uptake versus time. At pressures close to the saturation point, special attention was paid to avoid water vapour condensation. From the mass gains (noted  $M$  expressed in g of water per g of fibre sample, eq 3) at the equilibrium state for each water activity, the water sorption isotherm was then plotted. The inaccuracy of mass uptakes at sorption equilibrium was estimated to be less than 3%.

$$M = \frac{m_{eq} - m_0}{m_0} \times 100 \quad (\text{Eq. 3})$$

With  $m_{eq}$  and  $m_0$  are the mass at equilibrium state and the initial mass, respectively. The water vapour sorption isotherms were fitted using the Park model (eq. 4) which displays a multi-sorption mode through three terms with five mathematical parameters to be determined. The three contributions to the sorption are defined as a function of the water activity range: 1) at low water activities, Langmuir-type sorption is performed at the surface of specific sites or microcavities; 2) at medium water activities, Henry's law sorption is relative to a random water adsorption through a dissolution/diffusion mechanism; and 3) at high water activities, a clustering reaction of water molecules is observed.

$$M = \frac{A_L b_L}{1 + b_L \cdot a} \cdot a + k_H \cdot a + n \cdot K a \cdot k_H^n \cdot a^n \quad (\text{Eq. 4})$$

Where  $a$  defines the water activity,  $A_L$  is the average concentration of water molecules in the Langmuir sites,  $b_L$  is the affinity constant between water molecules and the Langmuir sites,  $k_H$  is the Henry's law constant, «  $K_a$  » is the equilibrium constant associated with the water aggregation reaction and  $n$  is the mean number of water molecules constituting the aggregates.

To evaluate the goodness of the mathematical fit of this model, the mean relative deviation modulus, noted MRD (expressed in %), was calculated by using the root sum square method between the fit and the experimental data:

$$MRD = \frac{100}{N} \sum_i^N \left| \frac{m_i - m_{pi}}{m_i} \right| \quad (\text{Eq. 5})$$

where  $m_i$  is the experimental mass at sorption equilibrium,  $m_{pi}$  the predicted mass resulting from isotherm modelling and  $N$  is the number of experimental data. Widely-adopted in the literature, a value below 10% indicate a good fit as mentioned by Lomauro [51]. A non-linear regression analysis of model parameters by Tablecurve 2D software was carried out.

### 3. Results:

#### 3.1 Comparison of different milling routes to produce fine flax powders

First, we compare the different milling routes used to produce fine ground powder. Continuous milling processes that generate impact (impact mill) and shear (centrifugal mill) mechanical stresses have been investigated. The resulting ground powders are named FLAX 1 - 4 (Fig 1) and have been thereafter characterised in terms of size and shape in comparison to raw flax.

Figure 2 shows the distribution of particle size after each milling step obtained by laser granulometry measurement; in addition and for each batch, SEM images of milled fibres are shown, and the fibres lengths and diameters obtained by quantitative morphological analysis are indicated. One can notice that the particle size distribution of raw flax measured by laser diffraction exhibits three modes at approximately 709  $\mu\text{m}$ , 138  $\mu\text{m}$  and 30  $\mu\text{m}$  (figure 2). It is interesting to note that the value of mode 1 and 3 are comparable to the length ( $707 \mu\text{m} \pm 15\mu\text{m}$ ) and the diameter ( $37 \mu\text{m} \pm 0.1 \mu\text{m}$ ) of RAW FLAX fibres measured by image analysis. As the mathematical models used in laser diffraction assumes that particles are spherical that is far from the case of flax fibre ( $L/D=19 \pm 0.4$ ), the laser diffraction is *a priori* not the most suitable technique to measure the particle size of the raw flax fibres. Nevertheless, the resulting particle size distribution can bring interesting elements to follow the influence of the milling process on the characteristic length of the ground powder.

In Figure 2, we can also note that the different milling routes tested produced fine particles with the appearance of new modes around 91 and 1  $\mu\text{m}$ . As the distribution is expressed in % volume, the number of finest particle (1  $\mu\text{m}$ ) is significant even if the proportion of the peak is weak in comparison to the others. The mode around 709  $\mu\text{m}$  shifts to the left from FLAX 1 to FLAX 3. For FLAX 4 this mode has disappeared evidencing that the totality of

original flax fibres have been cut and morphologically modified by the milling process. The SEM morphological characterisation confirms the results obtained with laser diffraction. Only a slight evolution in the fibre diameter is observed.

The length of the RAW FLAX decreases slowly with each subsequent milling step, and in comparison to RAW FLAX, the length of FLAX 4 is shorter by a factor of 2.7 ( $=707/262$ ). This could be related to the fact that grinders have sieves with holes greater than the diameter of the fibre. Thus, particles can pass through the sieve holes in the longitudinal direction without being cut. **As a result, the residence time is weak. Thus, even if energy is transmitted during impact between the particles and the rotor and the sieve play an important role (due to high rotation speed), the total milling energy (function of the impact energy and the residence time) is not sufficient to effectively reduce the particle size. Note that the sieve employed in the second milling step (100  $\mu\text{m}$  for the impact mill and 120  $\mu\text{m}$  for the centrifugal mill) are the smallest sieves available for this technology. Indeed, sieves with holes smaller than 100  $\mu\text{m}$  are not adapted for dry grinding of materials because of clogging effects due to the increase in cohesion forces which becomes prominent as particle size decreases. Clogging effect leads to stagnation of the milling process, to high temperatures, and increase in torque , and consequently inducing damage to the machine.**

In addition, RAW FLAX is mainly composed of cellulose, an assembly of linear polymers of beta-1-4-linked-D-glucopyranose units arranged in microfibrils through hydrogen bonds and van der Waals forces. Microfibrils combine to form fibrils which are aligned in the longitudinal direction and leads to an anisotropic structure with higher mechanical properties in the longitudinal direction (Young's modulus, tensile strength, Poisson coefficient, etc.) than in the transverse one. As a result, a significant amount of the energy injected by the grinders generating shear stress and impact is involved in the fibre length reduction but also to dissociate the fibre; this conjugated effect leads to a defibrillation process as observed in the SEM observation of FLAX 1 to FLAX 4. **Thus the way in which the energy is transmitted is also essential in the comminution process.**

**In order to increase the energy applied onto the material, the multiplication of milling passes could be considered. However, in view of the scale-up of the process for industrial applications, it may not be an option because of the increase in production costs and the difficulty in practically implementing this.**

As the technologies used in this first part do not produce fine flax particles, a vibratory ball mill applying compression and attrition as the principal mechanical stresses was then employed. This device is a batch mill and the evolution of the comminution process was followed by withdrawing samples at different milling times (Fig 1). The corresponding particle size distributions, obtained by laser granulometry, are presented in Figure 3. The first mode at 709  $\mu\text{m}$ , related to the length of the fibres, is still present on the particle size distribution and decreases slowly with milling time. This decrease is accompanied by an increase of the proportion of fine particles below 200  $\mu\text{m}$  and more particularly by the appearance of two modes centred at 91 and 1  $\mu\text{m}$ ; as seen previously for the continuous mills. However for longer milling times of 17H00 and 23H00, a new population around 15  $\mu\text{m}$  appears. It is worth noting that this value corresponds to the generally-accepted mean diameter of elementary flax fibres [52]. This new population shows that the ball milling process is able to drastically reduce the particle size of flax fibres whereas this was not possible with the continuous milling equipment.

Figure 4 shows the evolution of the main particle size descriptor ( $d_{10}$ ,  $d_{50}$ ,  $d_{90}$ ) as a function of milling time. Interestingly, 4 zones could be distinguished on the graph. In the first one, up to 60 mins of milling,  $d_{10}$  and  $d_{50}$  decrease rapidly and  $d_{90}$  more slowly; then, in the second one, the tendency reverses with a greater slope for  $d_{50}$  than for  $d_{90}$  related to the persistence of the peak at 709  $\mu\text{m}$  (Figure 3). From 8 hours, the slopes of  $d_{50}$  and  $d_{90}$  decrease highlighting a slow-down of the milling process.

This phenomenon have been previously described in literature especially for ball milling and is often attributed to cushioning effects due to the production of fine particles during the milling process which surround the coarser particles and amortize the transmission of the stress [53,54]. Another explanation is related to the reduction in the number of defects when particle size decreases. Indeed, fracture paths, responsible for the comminution of the particles, are initiated in weak areas of the materials, propagating through the defects. As a results, the probability of the presence of defects inside a particle decreases with particle size. The energy necessary to initiate fracture increases, leading to a slowing-down of the kinetics of comminution [55]. Finally in the last zone, we observe a slight increase of  $d_{50}$  and  $d_{90}$  that could be related to agglomeration phenomena observed in dry ball milling and described for example by Guzzo et al. investigating the milling of limestone [56]. These are known to be competitive comminution processes and can also responsible for the slow-

down observed. Interestingly, we also observed in figure 3 that the slow-down is correlated to a strong modification in the shape particle size distribution. In the following sections, we will investigate the other chemical and physical modifications that can be related to the described transitions.

### 3.2 Evolution of flax fibre morphology during ball milling

Figure 5 shows the evolution of fibre aspect ratio ( $L/D$ ), length ( $L$ ) and diameter ( $D$ ) with milling time. As expected, the ball milling process has a strong impact on the morphology of the fibre elements. Two behaviour domains are clearly evidenced. The aspect ratio ( $L/D$ ) of the fibre elements decreases sharply and almost linearly with time of ball milling up to 8 hours. This strong decrease in the fibre elements'  $L/D$  is mostly connected to the evolution of the fibre elements length, as the average diameter remains constant up to 7H00 (420 min), above 35  $\mu\text{m}$ . Above 8H00 (480 min), the aspect ratio decreases only slightly, to reach a plateau of around 5. This is largely due to a gradual reduction in the fibre element diameter above 8H00 of ball milling time, to a value of under 30 $\mu\text{m}$  after 23H00 of ball milling (1380 min). Fibre element length seems to reach somewhat of a plateau after 8H00 of ball milling; this is presumably related to the critical distance between structural defects, such as kink bands. Interestingly, this dual mode phenomenology was already reported for element evolution in melt processing [57] and the drivers of the decrease in length versus decrease in diameter were investigated. This evolution is likely under the control of interconnected variables such as the processes parameters (i.e during twin-screw extrusion) [58], intrinsic properties of the materials [59] and also the moisture content present in the natural fibre [60].

### 3.3 Evolution of the chemical composition of flax fibres during ball milling

The monosaccharide (also known as sugar or carbohydrate) content of the BM samples were analyzed by a conventional biochemical procedure. The total monosaccharide content is close to 80% of the fibre elements dry matter (DM), with an average 69% of the DM represented by glucose monosaccharide. Assuming that all this glucose belongs to cellulose, then both the non-glucosidic monosaccharide (galacturonic acid, and neutral monosaccharides mannose, xylose, galactose, rhamnose, arabinose and fucose) and the cellulosic compartment quantified are in the range of the reported values in the literature [52] for flax technical fibres. The panel of non-glucosidic monosaccharide is shown in Figure

6 and appears constant for all ball milling processing times (2H20 to 23H00). In contrast, the main component of the fibre elements, cellulose, assumed to be represented by glucose, does evolve with ball milling time (Fig.6). While there is only a slight decrease in cellulose content up to 5H30 of processing, a drastic loss occurs between 10H00 and 23H00 with a drop from 67% to 60% cellulose content of the fibre elements dry mater.

### 3.4 Evolution of cellulose crystallinity of flax fibres during ball milling

The diffraction pattern of cellulose I (Fig. 7a) includes five major reflections for the crystalline phases at  $2\theta \approx 15^\circ$  (101 diffraction plane),  $17^\circ$  ( $10^{-1}$ ),  $21^\circ$  (021),  $22.5^\circ$  (002) and  $34.5^\circ$  (040), with the amorphous phase observed at  $2\theta \approx 18.5^\circ$ [61]. These reference peaks were used to analyse the XRD spectra of the various flax fibre samples (Fig. 7a). All samples exhibit a primary peak at  $2\theta \approx 22.5^\circ$  corresponding to the crystalline 002 plane of cellulose I, however the peak is sharp and distinct for RAW FLAX, FLAX BM 2H20, and FLAX BM 10H00 but very broad for FLAX BM 17H00 and FLAX BM 23H00. In addition, RAW FLAX and FLAX BM 2H20 exhibit the 101 and  $10^{-1}$  secondary peaks (less distinct in the case of FLAX BM 10H00), while these peaks are not discernible in the diffraction spectra for FLAX BM 17H00 and FLAX BM 23H00. Generally, these two peaks are more separated when the **rate of crystallinity** of cellulose is high [62]. In case of important amount of amorphous polymers such as pectins, lignin, hemicelluloses or amorphous parts of cellulose, the two peaks are overlapping and difficult to deconvolute. Here, the amorphous phase (trough between the primary and secondary crystalline peaks) is also very clear in RAW FLAX and FLAX BM 2H20. No shift in diffraction peaks is observed. The noted qualitative observations suggest a reduction in crystallinity (increase in level of disorder) of the fibres. Calculations using Eq.1 reveal that indeed, crystallinity of the material deteriorates substantially with duration of ball milling. Specifically, while the powdered RAW FLAX (0h ball milling) has a crystallinity of 72.0%, consistent with literature data [50, 63], crystallinity reduces to 56% after 10H00 of ball milling and down to 16.6% after 23H00 of ball milling. Interestingly, this reduction in crystallinity appears to be linearly related to milling time (figure 7b) with a strong negative regression coefficient between decrease of crystallinity and process duration.

### 3.5 Evolution of thermal properties of flax fibres during ball milling

Table 1 shows the impact of milling time on thermal properties of flax fibres. The thermal behaviour of plant fibres has already been described in literature [64]; it can be influenced by their structure and composition. One can generally observe three peaks in the derivative curve and three mass losses are associated to these peaks. For flax fibres, they are attributed to the release of water, the degradation of cellulosic substances (amorphous and crystalline cellulose), and the degradation of non-cellulosic substances, such as lignin, hemicelluloses, and sugar mallard derivatives. In the present work several tendencies may be underlined (Table 1). First, increased water loss was noticed with increase in milling time. As observed in SEM images (Figure 4), milling induces strong alteration of fibre integrity (especially visible after 8H00) and probably enhances water accessibility to the different fibre cell wall layers, especially the S2 layer, and potential middle lamellae residues which are pectin enriched and potentially responsible for a significant water uptake. Moreover, the thermo-mechanical damages suffered by plant cell walls are in favour of better water accessibility to the fibre micro-porosities, located inside the cell walls or between structural layers and responsible for bound water storage. For raw fibres (RAW FLAX), this access is limited, probably restricted to defects, such as kink bands, regions; mainly free surface water is assumed to be accessible in this case.

Peak II exhibits a significant rise of around 6 wt% after the 2h20 heating, then its value remains stable. The increase is probably due to the higher accessibility to cellulosic substances inducing the degradation of the whole part of these components at this step; this thermal degradation may be potentially delayed towards higher temperature when fibres are undamaged. Simultaneously, one can observe a regular decrease in the onset temperature of peak II; higher milling times lead to an increase in amorphous fraction of cellulose, which are more thermosensitive than crystalline cellulose.

Finally, the third peak is generally associated to thermo-resistant polymers, like lignin, and longer cellulose chains of high degree of polymerisation. Those  $\alpha$ -cellulose are thermodynamically more stable, and could be part of peak III. We hypothesise that ball milling progressively depolymerises the more stable cellulose, evidenced by a progressive decrease in the weight loss. Consequently, the maximum temperature of peak III would decrease, which is what we find. This hypothesis is strongly supported by biochemical data,

and also by the decrease in crystallinity of cellulose with increasing ball milling time (see Fig 7b).

### 3.6 Change in water vapour sorption properties of flax fibres during ball milling

Water vapour sorption measurements were performed on RAW FLAX fibre and the various FLAX BM samples to measure and analyse their differing sorption kinetics.

The water vapour isotherm curves, as plotted in Fig. 8, represent the water mass gain (expressed in %) at the sorption equilibrium state as a function of water activity. The sigmoidal shape of the isotherm curve of RAW FLAX is maintained after ball milling. Generally, hydrophilic or natural substrates display this kind of profile. This conforms to a three-mode sorption profile: i) an upswing of the water mass gain concave to the activity axis at low water activity ( $a < 0.2$ ) is assigned to Langmuir's mode of sorption, ii) a linear part at intermediate activity attributed to Henry's law sorption, followed by iii) a sharp rise of mass gain with further increase in water activity ( $a > 0.7$ ), describing the aggregation phenomena of the absorbed water molecules in the sample. The isotherm curves were mathematically fitted by applying the Park model (Eq.4), which is suitable for modeling sigmoid profiles obtained for natural substrates [65]. The Park model incorporates three contributions to water sorption from three terms with five adjustable parameters, as described in Section 2.8. The values of the parameters are presented in Table 2.

Within the range of water activities applied, and particularly for water activities over 0.3, the increase in  $k_H$  with duration of ball milling indicates that the water mass gain increases with the duration of ball milling. The highest water uptake was measured for the most intensely milled fibre. This first observation leads us to believe that the access of absorbed water molecules to polar functional groups, allowing interactions through hydrogen bonding, is higher after ball milling. This is backed by our previous observations that ball milling modifies the raw fibre structure by mechanical damage from stress application - mostly shearing, impact and compression in the case of ball milling. The overall increase of water sorption with milling time can be related to two direct effects of the mechanical damages induced by milling on the fibres' structure. The fibre integrity is also strongly altered with a reduction in fibre size and partial delamination in fibre layers. This has facilitated the access of water to new binding sites in the different fibre layers, especially the internal pectin-enriched layers. This induces a higher incoming water concentration, and hence a water uptake, which can

be correlated to the higher water mass gain at low water activities ( $<0.2$ ) owing to an increase of the incoming water-polar functions interactions, such as hydroxyl functions of hemicellulose and cellulose.

The  $A_L$  value increase is indicative of an increase in water solubility in treated fibres. Such effects can lead to an increase in free volume and of polymer chain mobility; all the more since the fibres are shortened by ball milling. Consequently, the classical water plasticization phenomenon occurs, and water mass gain accordingly increases at intermediate water activities. This trend is supported by a higher weight loss for the peak II in TGA, as observed in table 1, reflecting higher accessibility to cellulosic substances in fibres, and hence higher accessibility to polar sorption sites to initiate hydrogen bonding with water molecules, which is also evidenced by the  $K_H$  value increase. Such effects are larger for longer durations of ball milling. This effect can be also associated with better water accessibility to the fibre lumen providing a location for free water storage. This additional direct effect of ball milling can partly explain the rise in the water mass gain at high water activities. The second possibility concerns the water aggregation occurring from the first layer of incoming water linked to polar functions of fibres by hydrogen bonding. Both trends can lead to the formation of water clusters within the fibre samples. This can be related to the increase in  $n$  and  $K_a$  values, indicative of the entrance of water molecules during clustering phenomenon. With ball milling duration, a reduction of  $n$  value is observed, suggesting lower-size water aggregates. This interesting result can be interpreted by the reduction of fibre size and the partial fibre delamination which favour a homogeneous distribution within the sample of the sorbed water molecules in increasing concentration, leading to a lower mean size of the water aggregates.

### 3 Discussion

In this work we studied a large number of morphological, structural and process related parameters. Figure 9 summarizes the various analyses and provides a link between the analyses described in the previous sections. In order to not overload the graph and make it more readable, only three milling times, selected for their importance in the changes noted, were chosen. We can see in Figure 9 that the main parameters impacted in the first grinding phase (between 0 and 10 hours) are mainly the length of the fibres (about -70%), the

crystallinity index (-26%) as well as the water absorption capacity of the ground fibres with an increase of about 20 to 30% of this water absorption capacity by the fibre walls. The modifications induced by ball grinding during this first phase are therefore essentially morphological, in particular a severe drop in length. This damage and fractionation of the fibres inevitably leads to an increase in the potential sites of water entry into the walls, which has a very significant influence on their water absorption capacity. At the same time, and probably under the action of water which induces mobility of structural polymers, the nature and organization of cellulose is changing (vis. amorphisation).

This relationship between the hygroscopic behaviour of the flax cell walls and crystallinity continues in the second phase of milling, between 10 and 23 hours, with a steady increase in water mass gain of the fibre samples between water activities of 0.1 and of 0.6 and also the first peak of TGA, representative of the water content of the cell walls. At the same time, this severe grinding induces an additional drop in crystallinity of about 50%. This is illustrated by Figure 10 which shows the evolution of the sorbed water content of the raw flax fibre walls as a function of crystallinity.

An interesting correlation can be noted with the three water indicators considered. The most pronounced correlation is obtained between the crystallinity of the flax walls and the water content at the water activity equal to 0.6. As discussed earlier, the crystallinity of the fibre samples decreases with increasing duration of ball milling. This is a key factor in understanding the change in sorption capacity because the sorption of molecules occurs in the amorphous phase of a substrate, the crystalline phase being assumed to be an almost impermeable area to permeants [66] and so accordingly acting as obstacles to the diffusion of these permeants. This change in crystallinity implies the presence of a larger amorphous phase, explaining also higher water sorption capacity as the duration of ball milling increases.

Other than the clear influence on cellulose crystallinity, the ball milling process has a complex, unclear influence on cell wall polysaccharides. On the one hand, the non-glucosidic monosaccharides remained at a fairly constant fraction of the dry mass (Fig 6) for all processing times. Surprisingly, only the glucosidic content, assumed as cellulose, decreased by around 10% between 10H00 and 23H00 of ball milling time. The apparent loss of cellulose

is hypothesized to be both due to a conversion of the glucose moieties into other chemicals, i.e. small glucan chain further turned into 1,6-anhydroglucan by non-atmospheric plasma [67], products that we could not detect with the analytical procedure followed herein. A second hypothesis to explain the loss of cellulose is its conversion into volatile organic compounds [68]. Supporting our observation of this specific degradation of cellulose and not non-glucoside monosaccharides, we find in wood literature that ball milling affects only cellulose (with an optimal time of processing), without substantially modifying the lignin structure, which is present in low fractions in flax fibers studied herein. Further, in an aim to extract lignin-carbohydrate complexes (LCC) assisted by solvent, Li et al. [69] efficiently extracted LCC after ball milling while keeping stable or slightly increased content of non-glucosidic monosaccharides between 12 or 24h of ball milling. By molecular weight analysis, severe depolymerization of the original cellulose has been reported for wood after ball milling, and this technique also shows coinciding and uniform distribution curves of hemicelluloses (non glucosidic monosaccharides) before and after ball milling [70]. Such findings reinforce our observation that the non-glucosidic monosaccharides are less impacted than their cellulosic counterparts by ball milling, in contrast to mild or severe chemical processes [71].

In general, these different evolutions, induced by high shear during milling, are strongly linked to morphological changes which, by increasing water absorption, facilitate and accelerate structural damage to plant walls. **In addition, the morphometry of the particles follows a non- monotonic evolution. Indeed, after substantial length reduction up to 10 hours of grinding, thereafter only slight diminution happens; the length has reached a critical threshold level (Figure 6). The same trend is observed for particle diameter, with a threshold limit equivalent to the elementary fibre diameter (Fig. 11).** However, this modest morphological evolution between 10 and 23 hours does not prevent crystallinity or water absorption capacity from continuing to evolve. Structural changes are continuing in the longer term, probably due to the temperature induced by the grinding process but also due to the progressive effect of water penetration into the core.

**In view of the different modifications highlighted in this work, an important question remains: are these modifications desirable? It is not easy to answer this question as the**

properties targeted for the ground powder can vary significantly according to the end-use application. Generally speaking, intense milling significantly increases the reactivity of the powder by increasing the specific surface area. In addition, the modification of other properties can be an asset to increase the potential of the powder for several applications. For example, in the case of bioethanol production, the reduction in cellulose crystallinity leads to a higher efficiency in enzymatic hydrolysis reaction [31]. In a similar way, the increase in water absorption capacity could enhance the potential of disintegration of the polymeric matrix by the biomass in planned obsolescence agro-composites [72]. However, the same increase can also be damaging, as rapid water uptake leads to a decrease of the energetic potential of the biomass powder in energetic applications as direct combustion in engine [9]. This also increases the cohesion effect which complicates the implementation of the powder in the downstream process step. We can cite for example the production of enriched fraction with electrostatic separation processes [73]. In other words, if an intense milling step could increase the reactivity of the powder, it also influences its stability. Thus for a given application, where intense milling is required the determination of the optimal milling time needs to be realized based on a best compromise between the targeted end-use properties and the undesirable, induced ones. Finally, the determination of the optimal milling time may need to be based on the energetic cost of the operation and it is interesting to correlate the modifications highlighted by the milling to the energy supplied during ball grinding (Fig. 11). Several grinding laws have been proposed to predict the energy cost of a milling process. The best known are the ones by Von Rittinger, Kick and Bond which all express the energy as a function of the variation of the fineness of the product. In particular, the Von Rittinger model [74] states that the specific energy  $E_m$  (energy per unit of mass) is directly proportional to the creation of specific surface area (see Eq. 6) :

$$E_m = K_r(S_{p2} - S_{p1}) = K_r \cdot S_a \quad (\text{eq 6})$$

with  $K_r$  a constant depending both on the material to grind and the grinder, and  $S_{p1}$  and  $S_{p2}$  the specific surfaces of the particle before and after breakage. In case of coarse milling of lignocellulosic materials, this model been validated for wood chip, alpha chops and pellet milling [24, 75]. Here, the milling energy has been calculated from the active operating power of the vibratory ball mill multiplied by the milling time, and the specific surface area of the ball milled flax powder was determined from the particle size distribution. Figure 11 presents the evolution of milling energy with the specific surface area created (Specific

surface area of the sample minus those of the raw flax) together with a linear fit of the experimental data according to the Von Rittinger models. One can note that the Von Rittinger model fits very well the experimental data with a correlation coefficient  $R^2$  greater than 0.98 suggesting that the grinding limit is not yet reached after 23H00 of milling. Indeed, when this limit is reached, a substantial decline of the slope would be observed [7] reflecting that the energy supplied by the grinder would not be used to create new surfaces but would be rather associated with thermal or agglomeration phenomena [53].

#### **4 Conclusion**

The objective of this work was to study the impact of milling on the properties of flax fibres, which are considered as a model biomass due to their high crystalline cellulose content and their hierarchical multilayer structure.

After a comparative work between different various grinding techniques, ball milling was selected because of its efficiency and ability to provide a wide range of particle size distributions. Morphological measurements carried out for milling times up to 23 hours have shown a marked decrease in the length and aspect ratio of the fibres; the diameter is less affected because of the smaller magnitude of this parameter due to the initial fineness of the fibres and the diameter of the elementary fibres, which constitutes a lower limit.

In terms of structure and composition of the flax cell walls, major modifications have been highlighted; it appears that mainly cellulose is impacted by the process. A steady decrease in glucose level and also in the crystallinity of cellulose has been observed with ball milling duration. This modification of cellulose is favoured by thermomechanical alteration highlighted by SEM imaging and corroborated by the sorption behaviour of the cell walls. Increasing accessibility of water has been shown by DVS and ATG, caused by the increase in amorphous regions. Thus, the milling of biomass, for example for composite reinforcement applications, has a significant impact on its structural and morphological properties. Consequences are also to be expected in terms of mechanical performance and reinforcement, in particular due to the loss of fibre integrity and the drastic evolution of their morphology.

## Acknowledgment

Jacqueline Vigouroux (INRA, Nantes) and Cécile Sotto from the plant transformation platform of the JRU IATE are gratefully acknowledged for their helpful advice and assistance in carbohydrate analysis and grinding experiments respectively. The authors also thank the French national research Network 'GDR 3710 INRA/ CNRS SYMBIOSE – Synthons et matériaux biosourcés', for its financial support.

## Reference list

- [1] R. Ho, M. Naderi, J.Y.Y. Heng, D.R. Williams, F. Thielmann, P. Bouza, A.R. Keith, G. Thiele, D.J. Burnett, Effect of Milling on Particle Shape and Surface Energy Heterogeneity of Needle-Shaped Crystals, *Pharmaceutical Research*, 29 (2012) 2806-2816.
- [2] C. Frances, N. Le Bolay, K. Belaroui, M.N. Pons, Particle morphology of ground gibbsite in different grinding environments, *International Journal of Mineral Processing*, 61 (2001) 41-56.
- [3] E. Kaya, R. Hogg, S. Kumar, Particle Shape Modification in Comminution, *KONA Powder and Particle Journal*, 20 (2002) 188-195.
- [4] R. Li, M. Qin, C. Liu, Z. Chen, X. Wang, X. Qu, Particle size distribution control and related properties improvements of tungsten powders by fluidized bed jet milling, *Advanced Powder Technology*, 28 (2017) 1603-1610.
- [5] J.S. Kaerger, S. Edge, R. Price, Influence of particle size and shape on flowability and compactibility of binary mixtures of paracetamol and microcrystalline cellulose, *European Journal of Pharmaceutical Sciences*, 22 (2004) 173-179.
- [6] J.C. Motte, J.Y. Delenne, X. Rouau, C. Mayer-Laigle, Mineral–vegetal co-milling: An effective process to improve lignocellulosic biomass fine milling and to increase interweaving between mixed particles, *Bioresource Technology*, 192 (2015) 703-710.
- [7] C. Mayer-Laigle, N. Blanc, R. Rajaonarivony, X. Rouau, Comminution of Dry Lignocellulosic Biomass, a Review: Part I. From Fundamental Mechanisms to Milling Behaviour, *Bioengineering*, 5 (2018) 41.
- [8] C. Guizani, F.J. Escudero Sanz, S. Salvador, Influence of temperature and particle size on the single and mixed atmosphere gasification of biomass char with H<sub>2</sub>O and CO<sub>2</sub>, *Fuel Processing Technology*, 134 (2015) 175-188.
- [9] B. Piriou, G. Vaitilingom, B. Veyssi re, B. Cuq, X. Rouau, Potential direct use of solid biomass in internal combustion engines, *Progress in Energy and Combustion Science*, 39 (2013) 169-188.
- [10] M.A. Berthet, H. Angellier-Coussy, V. Chea, V. Guillard, E. Gastaldi, N. Gontard, Sustainable food packaging: Valorising wheat straw fibres for tuning PHBV-based composites properties, *Composites Part A: Applied Science and Manufacturing*, 72 (2015) 139-147.
- [11] P. Trivelato, C. Mayer, A. Barakat, H. Fulcrand, C. Aouf, Douglas bark dry fractionation for polyphenols isolation: From forestry waste to added value products, *Industrial Crops and Products*, 86 (2016) 12-15.

- [12] Y. Hemery, M. Chaurand, U. Holopainen, A.-M. Lampi, P. Lehtinen, V. Piironen, A. Sadoudi, X. Rouau, Potential of dry fractionation of wheat bran for the development of food ingredients, part I: Influence of ultra-fine grinding, *Journal of Cereal Science*, 53 (2011) 1-8.
- [13] H. Zeidler, D. Klemm, F. Böttger-Hiller, S. Fritsch, M.J.L. Guen, S. Singamneni, 3D printing of biodegradable parts using renewable biobased materials, *Procedia Manufacturing*, 21 (2018) 117-224.
- [14] R. Jauberthie, F. Rendell, S. Tamba, I. Cisse, Origin of the pozzolanic effect of rice husks, *Construction and Building Materials*, 14 (2000) 419-423.
- [15] A. Bourmaud, H. Dhakal, A. Habrant, J. Padovani, D. Siniscalco, M.H. Ramage, J. Beaugrand, D.U. Shah, Exploring the potential of waste leaf sheath date palm fibres for composite reinforcement through a structural and mechanical analysis, *Composites Part A: Applied Science and Manufacturing*, 103 (2017) 292-303.
- [16] P.F.H. Harmsen, W. Huijgen, L. Bermudez, R. Bakker, Literature review of physical and chemical pretreatment processes for lignocellulosic biomass, Wageningen UR - Food & Biobased Research, Wageningen, 2010.
- [17] S.V. Vassilev, D. Baxter, L.K. Andersen, C.G. Vassileva, An overview of the chemical composition of biomass, *Fuel*, 89 (2010) 913-933.
- [18] Q. Guo, X. Chen, H. Liu, Experimental research on shape and size distribution of biomass particle, *Fuel*, 94 (2012) 551-555.
- [19] K.L. Pickering, M.G.A. Efenfy, T.M. Le, A review of recent developments in natural fibre composites and their mechanical performance, *Composites Part A: Applied Science and Manufacturing*, 83 (2016) 98-112.
- [20] L.T.T. Vo, J. Girones, C. Beloli, L. Chupin, E. Di Giuseppe, A.C. Vidal, A. Soutiras, D. Pot, D. Bastianelli, L. Bonnal, P. Navard, Processing and properties of sorghum stem fragment-polyethylene composites, *Industrial Crops and Products*, 107 (2017) 386-398.
- [21] L. Chupin, D.d. Ridder, A. Clément-Vidal, A. Soutiras, E. Gineau, G. Mouille, S. Arnoult, M. Brancourt-Hulmel, C. Lapiere, D. Pot, L. Vincent, A. Mija, P. Navard, Influence of the radial stem composition on the thermal behaviour of miscanthus and sorghum genotypes, *Carbohydrate Polymers*, 167 (2017) 12-19.
- [22] D. Jones, C. Brischke, *Performance of Bio-based Building Materials*, Elsevier Science 2017.
- [23] H. Rezaei, C.J. Lim, A. Lau, S. Sokhansanj, Size, shape and flow characterization of ground wood chip and ground wood pellet particles, *Powder Technology*, 301 (2016) 737-746.
- [24] Z. Ghorbani, A.A. Masoumi, A. Hemmat, Specific energy consumption for reducing the size of alfalfa chops using a hammer mill, *Biosystems Engineering*, 105 (2010) 34-40.
- [25] Z. Miao, T.E. Grift, A.C. Hansen, K.C. Ting, Energy requirement for comminution of biomass in relation to particle physical properties, *Industrial Crops and Products*, 33 (2011) 504-513.
- [26] P. Karinkanta, A. Ämmälä, M. Illikainen, J. Niinimäki, Fine grinding of wood – Overview from wood breakage to applications, *Biomass and Bioenergy*, 113 (2018) 31-44.
- [27] A.S. Khan, Z. Man, M.A. Bustam, C.F. Kait, M.I. Khan, N. Muhammad, A. Nasrullah, Z. Ullah, P. Ahmad, Impact of Ball-Milling Pretreatment on Pyrolysis Behavior and Kinetics of Crystalline Cellulose, *Waste and Biomass Valorization*, 7 (2016) 571-581.
- [28] Y. Yu, H. Wu, Effect of ball milling on the hydrolysis of microcrystalline cellulose in hot-compressed water, *AIChE Journal*, 57 (2011) 793-800.

- [29] N. Stubičar, I. Šmit, M. Stubičar, A. Tonejc, A. Jánosi, J. Schurz, P. Zipper, An X-Ray Diffraction Study of the Crystalline to Amorphous Phase Change in Cellulose During High-Energy Dry Ball Milling, *Holzforschung - International Journal of the Biology, Chemistry, Physics and Technology of Wood*, 1998, 455.
- [30] M. Schwanninger, J.C. Rodrigues, H. Pereira, B. Hinterstoisser, Effects of short-time vibratory ball milling on the shape of FT-IR spectra of wood and cellulose, *Vibrational Spectroscopy*, 36 (2004) 23-40.
- [31] G.G.D. Silva, M. Couturier, J.G. Berrin, A. Buleon, X. Rouau, Effects of grinding processes on enzymatic degradation of wheat straw, *Bioresour Technol*, 103 (2012) 192-200.
- [32] R. Avolio, I. Bonadies, D. Capitani, M.E. Errico, G. Gentile, M. Avella, A multitechnique approach to assess the effect of ball milling on cellulose, *Carbohydrate Polymers*, 87 (2012) 265-273.
- [33] J.C. Tarafdar, S.C. Meena, S. Kathju, Influence of straw size on activity and biomass of soil microorganisms during decomposition, *European Journal of Soil Biology*, 37 (2001) 157-160.
- [34] D.J. Schell, C. Harwood, Milling of lignocellulosic biomass, *Applied Biochemistry and Biotechnology*, 45 (1994) 159-168.
- [35] S.N. Raghavendra, S.R. Ramachandra Swamy, N.K. Rastogi, K.S.M.S. Raghavarao, S. Kumar, R.N. Tharanathan, Grinding characteristics and hydration properties of coconut residue: A source of dietary fiber, *Journal of Food Engineering*, 72 (2006) 281-286.
- [36] C. Goudenhoft, T. Alméras, A. Bourmaud, C. Baley, The remarkable slenderness of flax plant and pertinent factors affecting its mechanical stability, *Biosystems Engineering*, 178 (2019) 1-8.
- [37] J.W.S. Hearle, P.J. Stevenson, Nonwoven Fabric Studies: Part III: The Anisotropy of Nonwoven Fabrics, *Textile Research Journal*, 33 (1963) 877-888.
- [38] T. Gorshkova, C. Morvan, Secondary cell-wall assembly in flax phloem fibres: Role of galactans, *Planta*, 223 (2006) 149-158.
- [39] G.J. McDougall, Isolation and partial characterisation of the non-cellulosic polysaccharides of flax fibre, *Carbohydrate Research*, 241 (1993) 227-236.
- [40] C. Morvan, C. Andème-Onzighi, R. Girault, D.S. Himmelsbach, A. Driouich, D.E. Akin, Building flax fibres: more than one brick in the walls, *Plant Physiology and Biochemistry*, 41 (2003) 935-944.
- [41] S. Alix, J. Goimard, C. Morvan, C. Baley, Influence of pectin structure on mechanical properties of flax fibres: a comparison between a linseed-winter variety (Oliver) and a fibrespring variety of flax (Hermès), in: H.A.V. Schols, R. G. F.; Voragen, A. G. J (2009), 99-98.
- [42] A. Bourmaud, M. Gibaud, C. Baley, Impact of the seeding rate on flax stem stability and the mechanical properties of elementary fibres, *Industrial Crops and Products*, 80 (2016) 17-25.
- [43] D.L. Easson, R. Anderson, H.S.S. Sharma, The sealed storage of moist flax with and without the use of chemical preservatives, *Annals of Applied Biology*, 125 (1994) 567-579.
- [44] S.B. Chemikosova, N.V. Pavlencheva, O.P. Gur'yanov, T.A. Gorshkova, The effect of soil drought on the phloem fiber development in long-fiber flax, *Russian Journal of Plant Physiology*, 53 (2006) 656-662.
- [45] C. Goudenhoft, D. Siniscalco, O. Arnould, A. Bourmaud, O. Sire, T. Gorshkova, C. Baley, Investigation of the Mechanical Properties of Flax Cell Walls during Plant Development: The Relation between Performance and Cell Wall Structure, *Fibers*, 6 (2018) 6.

- [46] D. Lee Black, M.Q. McQuay, M.P. Bonin, Laser-based techniques for particle-size measurement: A review of sizing methods and their industrial applications, *Progress in Energy and Combustion Science*, 22 (1996) 267-306.
- [47] E. Di Giuseppe, R. Castellani, S. Dobosz, J. Malvestio, F. Berzin, J. Beaugrand, C. Delisee, B. Vergnes, T. Budtova, Reliability evaluation of automated analysis, 2D scanner, and micro-tomography methods for measuring fiber dimensions in polymer-lignocellulosic fiber composites, *Compos. Pt. A-Appl. Sci. Manuf.*, 90 (2016) 320-329.
- [48] J.F. Thibault, Automatisation du dosage des substances pectiques par la methode au metahydroxydiphenyle, *Lebensmittel Wiss. Technol.*, 12 (1979) 247-251.
- [49] A.B. Blakeney, P.J. Harris, R.J. Henry, B.A. Stone, A simple and rapid preparation of alditol acetates for monosaccharide analysis, *Carbohydrate Research*, 113 (1983) 291-299.
- [50] A. Bourmaud, D. Siniscalco, L. Foucat, C. Goudenhooff, X. Falourd, B. Pontoire, O. Arnould, J. Beaugrand, C. Baley, Evolution of flax cell wall ultrastructure and mechanical properties during the retting step, *Carbohydrate Polymers*, 206 (2019) 48-56.
- [51] C.J. Lomauro, A.S. Bakshi, T. Labuza, Evaluation of food moisture sorption isotherm equations. Part II: Milk, coffee, tea, nuts, oilseeds, spices and starchy foods, *LWT - Food Science and Technology*, 18 (1985) 118-124.
- [52] A. Bourmaud, J. Beaugrand, D.U. Shah, V. Placet, C. Baley, Towards the design of high-performance plant fibre composites, *Progress in Materials Science*, 97 (2018) 347-408.
- [53] M. Capece, R. N. Dave, E. Bilgili, On the Origin of Non-linear Breakage Kinetics in Dry Milling, *Powder Technology*, Vol. 272, 2015, pp. 189-203.
- [54] M. Capece, E. Bilgili, R. Dave, Identification of the Breakage Rate and Distribution Parameters in a Non-Linear Population Balance Model for Batch Milling, *Powder Technology*, Vol. 208, 2011, pp. 195-204.
- [55] Blanc N., Frank X. , Mayer-Laigle C., Radjai F., Delenne J.Y, Peridynamics simulation of the comminution of particles containing microcracks, *EPJ Web Conf.*, 140 (2017) 07018
- [56] P.L. Guzzo, A.A.A. Tino, J.B. Santos, The onset of particle agglomeration during the dry ultrafine grinding of limestone in a planetary ball mill, *Powder Technology*, 284 (2015) 122-129.
- [57] A.S. Doumbia, M. Castro, D. Jouannet, A. Kervoëlen, T. Falher, L. Cauret, A. Bourmaud, Flax/polypropylene composites for lightened structures: Multiscale analysis of process and fibre parameters, *Materials & Design*, 87 (2015) 331-341.
- [58] F. Berzin, J. Beaugrand, S. Dobosz, T. Budtova, B. Vergnes, Lignocellulosic fiber breakage in a molten polymer. Part 3. Modeling of the dimensional change of the fibers during compounding by twin screw extrusion, *Composites Part A: Applied Science and Manufacturing*, 101 (2017) 422-431.
- [59] R. Castellani, E. Di Giuseppe, J. Beaugrand, S. Dobosz, F. Berzin, B. Vergnes, T. Budtova, Lignocellulosic fiber breakage in a molten polymer. Part 1. Qualitative analysis using rheo-optical observations, *Composites Part A: Applied Science and Manufacturing*, 91 (2016) 229-237.
- [60] J. Beaugrand, F. Berzin, Lignocellulosic fiber reinforced composites: Influence of compounding conditions on defibrization and mechanical properties, *Journal of Applied Polymer Science*, 128 (2013) 1227-1238.
- [61] S. Park, J.O. Baker, M.E. Himmel, P.A. Parilla, D.K. Johnson, Cellulose crystallinity index: measurement techniques and their impact on interpreting cellulase performance, *Biotechnology for Biofuels*, 3 (2010) 10.

- [62] V. Tserki, N.E. Zafeiropoulos, F. Simon, C. Panayiotou, A study of the effect of acetylation and propionylation surface treatments on natural fibres, *Composites Part A: Applied Science and Manufacturing*, 36 (2005) 1110-1118.
- [63] N.E. Zafeiropoulos, C.A. Baillie, F.L. Matthews, A study of transcrystallinity and its effect on the interface in flax fibre reinforced composite materials, *Composites Part A: Applied Science and Manufacturing*, 32 (2001) 525-543.
- [64] H.S.S. Sharma, G. Faughey, G. Lyons, Comparison of physical, chemical, and thermal characteristics of water-, dew-, and enzyme-retted flax fibers, *Journal of Applied Polymer Science*, 74 (1999) 139-143.
- [65] N. Follain, R. Saiah, K. Fatyeyeva, N. Randrianandrasana, N. Leblanc, S. Marais, L. Lecamp, Hydrophobic surface treatments of sunflower pith using eco-friendly processes, *Cellulose*, 22 (2015) 245-259.
- [66] Y. Tsujita, *The Physical Chemistry of Membranes*, in: Y. Osada, T. Nakagawa (Eds.) *Membrane Science and Technology*, Taylor & Francis 1992.
- [67] J. Delaux, C. Ortiz Mellet, C. Canaff, E. Fourré, C. Gaillard, A. Barakat, J.M. García Fernández, J.-M. Tatibouët, F. Jérôme, Impact of Nonthermal Atmospheric Plasma on the Structure of Cellulose: Access to Soluble Branched Glucans, *Chemistry – A European Journal*, 22 (2016) 16522-16530.
- [68] M. Claeys, B. Graham, G. Vas, W. Wang, R. Vermeylen, V. Pashynska, J. Cafmeyer, P. Guyon, M.O. Andreae, P. Artaxo, W. Maenhaut, Formation of Secondary Organic Aerosols Through Photooxidation of Isoprene, *Science*, 303 (2004) 1173.
- [69] J. Li, R. Martin-Sampedro, C. Pedrazzi, G. Gellerstedt, Fractionation and characterization of lignin-carbohydrate complexes (LCCs) from eucalyptus fibers, (2011) 43.
- [70] E. Sjöholm, K. Gustafsson, B. Eriksson, W. Brown, A. Colmsjö, Aggregation of cellulose in lithium chloride/N,N-dimethylacetamide, *Carbohydrate Polymers*, 41 (2000) 153-161.
- [71] B. Sharma, D.U. Shah, J. Beaugrand, E.-R. Janeček, O.A. Scherman, M.H. Ramage, Chemical composition of processed bamboo for structural applications, *Cellulose*, 25 (2018) 3255-3266.
- [72] Ndazi, B. and Karslon, S. (2011). Characterization of hydrolytic degradation of polylactic acid/rice hulls composites in water at different temperatures. *eXPRESS Polymer Letters*. 5. p119-131
- [73] Barakat, A., Mayer-Laigle C. (2017). Electrostatic Separation as an Entry into Environmentally Eco-Friendly Dry Biorefining of Plant Materials. *Journal of Chemical Engineering and Process Technology*, 8 (4).
- [74] P.R. Von Rittinger, *Lehrbuch Der Aufbereitungskunde: In Their Neuesten Entwicklung und Ausbildung Systematisch Darges Tellt*, Ernst & Sohn 1867.
- [75] M. Temmerman, P.D. Jensen, J. Hébert, Von Rittinger theory adapted to wood chip and pellet milling, in a laboratory scale hammermill, *Biomass and Bioenergy*, 56 (2013) 70-81.

### Table caption

**Table 1.** Thermo-gravimetric analysis on flax fibres and fines. Temperatures are indicated for inflection points of weight loss curves.

**Table 2.** Parameters of the Park model for the raw fibre and the treated fibres as a function of duration of ball milling.

### Figure Caption

**Figure 1 :** The different milling processes employed for the production of the flax powders.

**Figure 2 :** Particle size distribution obtained by laser granulometry and morphological characterization of the ground flax powder according to different milling route. SEM images of milled fibres are shown as well as the mean fibre lengths and diameters obtained by quantitative morphological analysis.

**Figure 3 :** Laser granulometry measurement: evolution of flax particle size distribution with the milling time.

**Figure 4 :** Evolution of main descriptors (d10, d50 and d90) of the particle size distribution as a function of time.

**Figure 5:** Evolution of the flax fibre morphology with milling time in the vibratory ball mill : aspect ratio (a) , length (b), diameter (c)

**Figure 6 :** Relative contents expressed as dry matter content of monosaccharides in the flax materials, unprocessed (RAW FLAX) and after increasing Ball Milling (BM) treatment over different durations (2H20; 5H30; 10H00 and 23H00).

**Figure 7:** a) XRD spectra for both the RAW FLAX and ball milled flax fibres as a function of process duration. For reference, the deconvoluted crystalline and amorphous peaks of cellulose I are also presented (from Park et al, 2010). b) The evolution in the crystallinity of the samples, calculated from XRD data, as a function of duration of ball milling (min).

**Figure 8 :** Water vapour sorption isotherms for the raw fibre and the treated fibres as a function of duration of ball milling. The isotherm curves were fitted from the Park model.

**Figure 9.** Evolution of the main parameters studied for the RAW FLAX samples, FLAX BM-10H00 and FLAX BM-23H00 .

**Figure 10:** Evolution of the hygroscopic and thermogravimetric behaviour of BM FLAX according to their crystallinity.

**Figure 11 :** Evolution of the milling energy with the specific surface area created

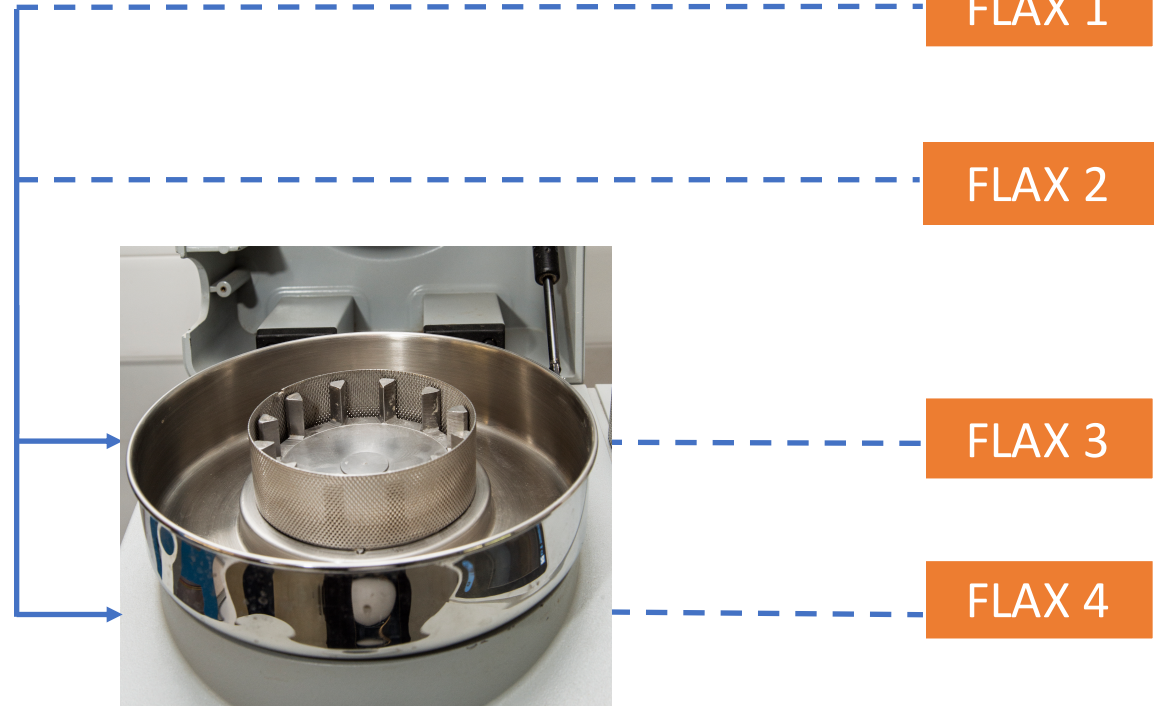
RAW FLAX  
1mm



Impact Mill  
UPZ

Screen:  
0.3 mm

Screen:  
0.1 mm



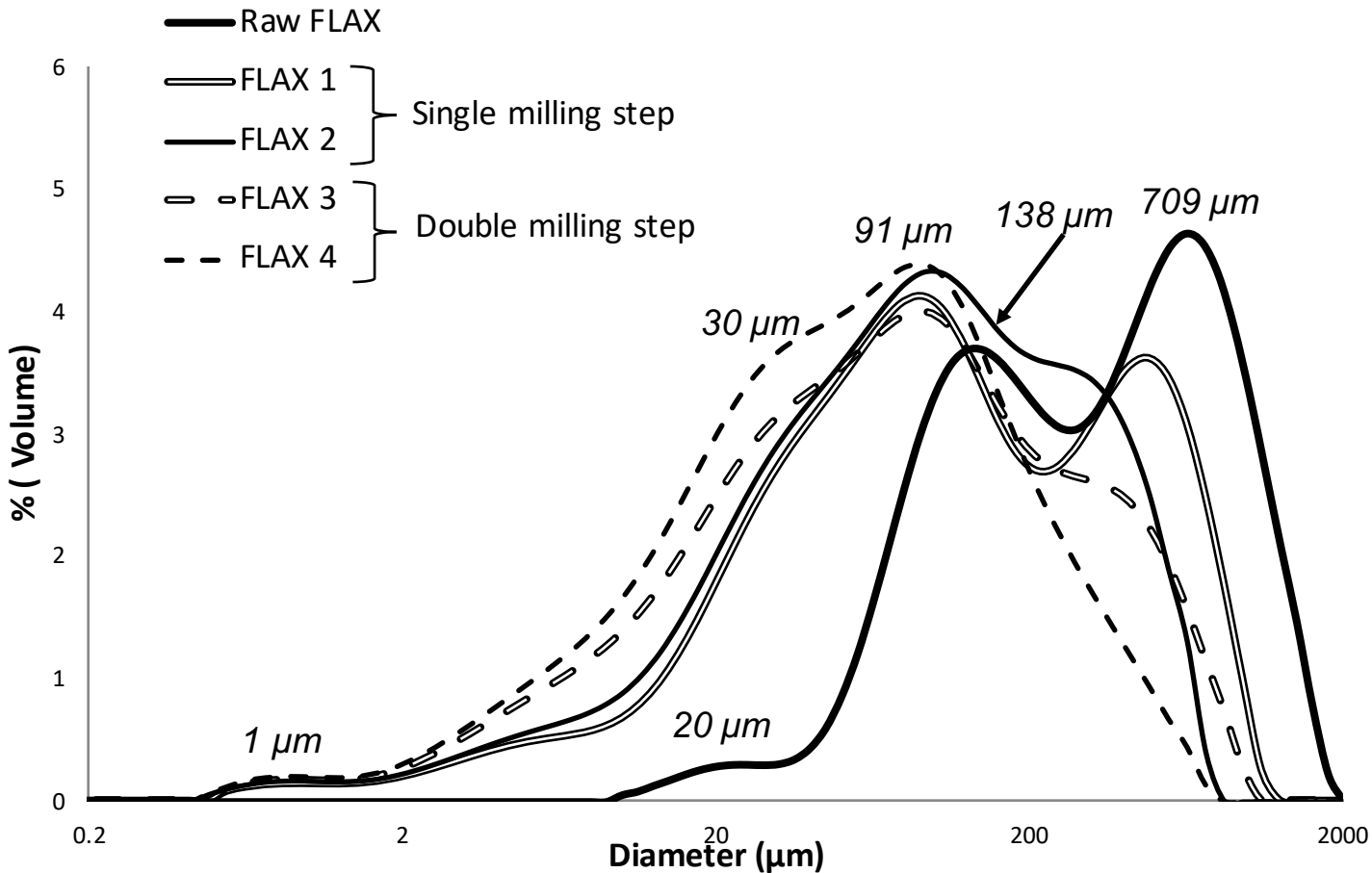
Centrifugal Mill  
SM200 (screen 0.12  
mm)



Ball Mill DM1

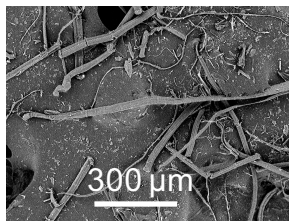
FLAX BM -

1H00  
2H20  
5H30  
7H00  
8H00  
10H00  
17H00  
23H00



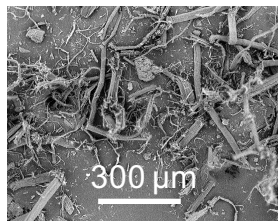
**Raw FLAX**

$L_w = 707 \mu\text{m}$   
 $D_w = 37 \mu\text{m}$   
 $L_w/D_w = 19$



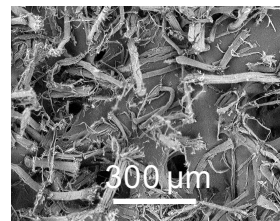
**FLAX 1**

$L_w = 659 \mu\text{m}$   
 $D_w = 32 \mu\text{m}$   
 $L_w/D_w = 21$



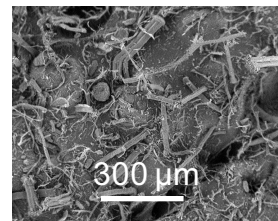
**FLAX 2**

$L_w = 368 \mu\text{m}$   
 $D_w = 30 \mu\text{m}$   
 $L_w/D_w = 12$



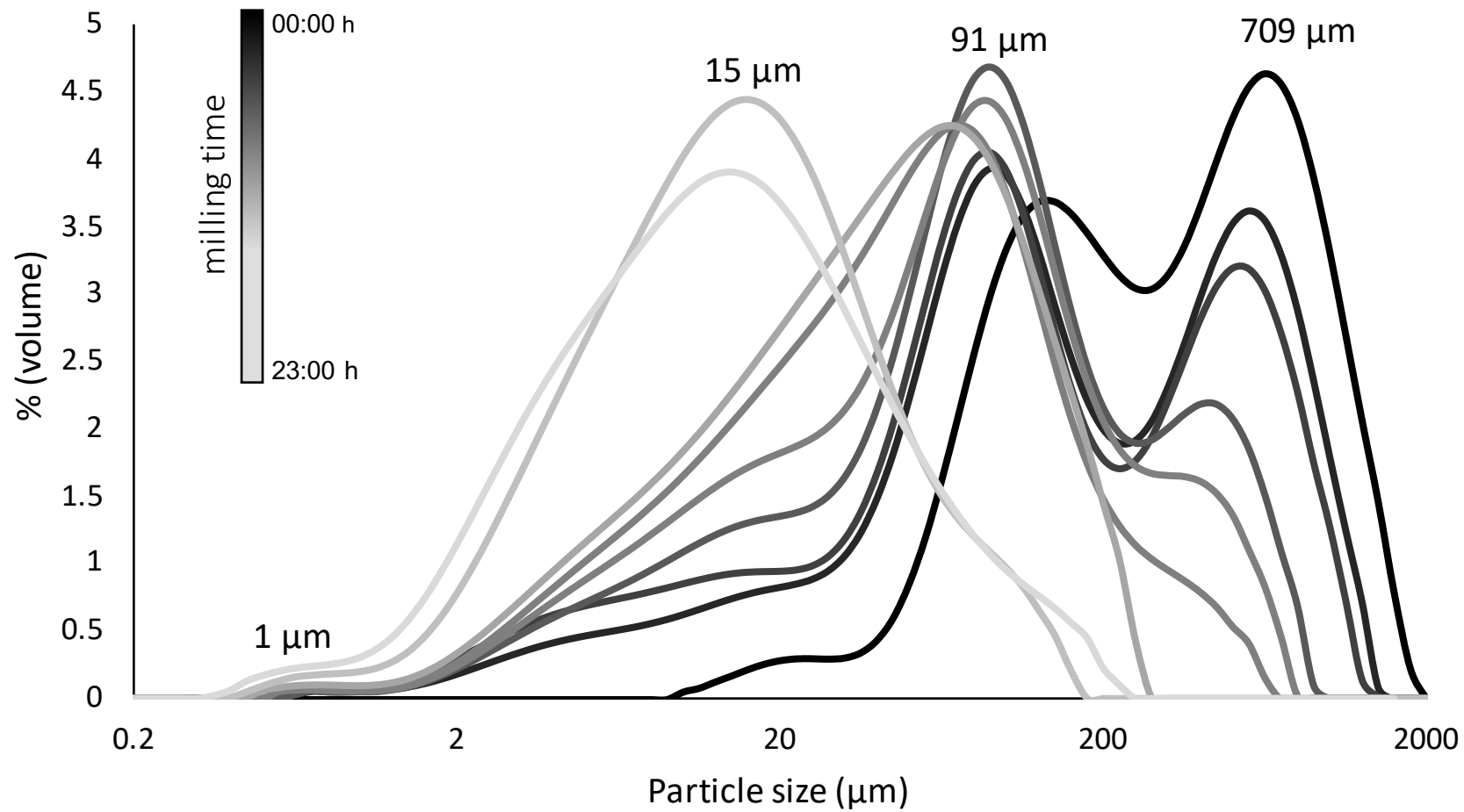
**FLAX 3**

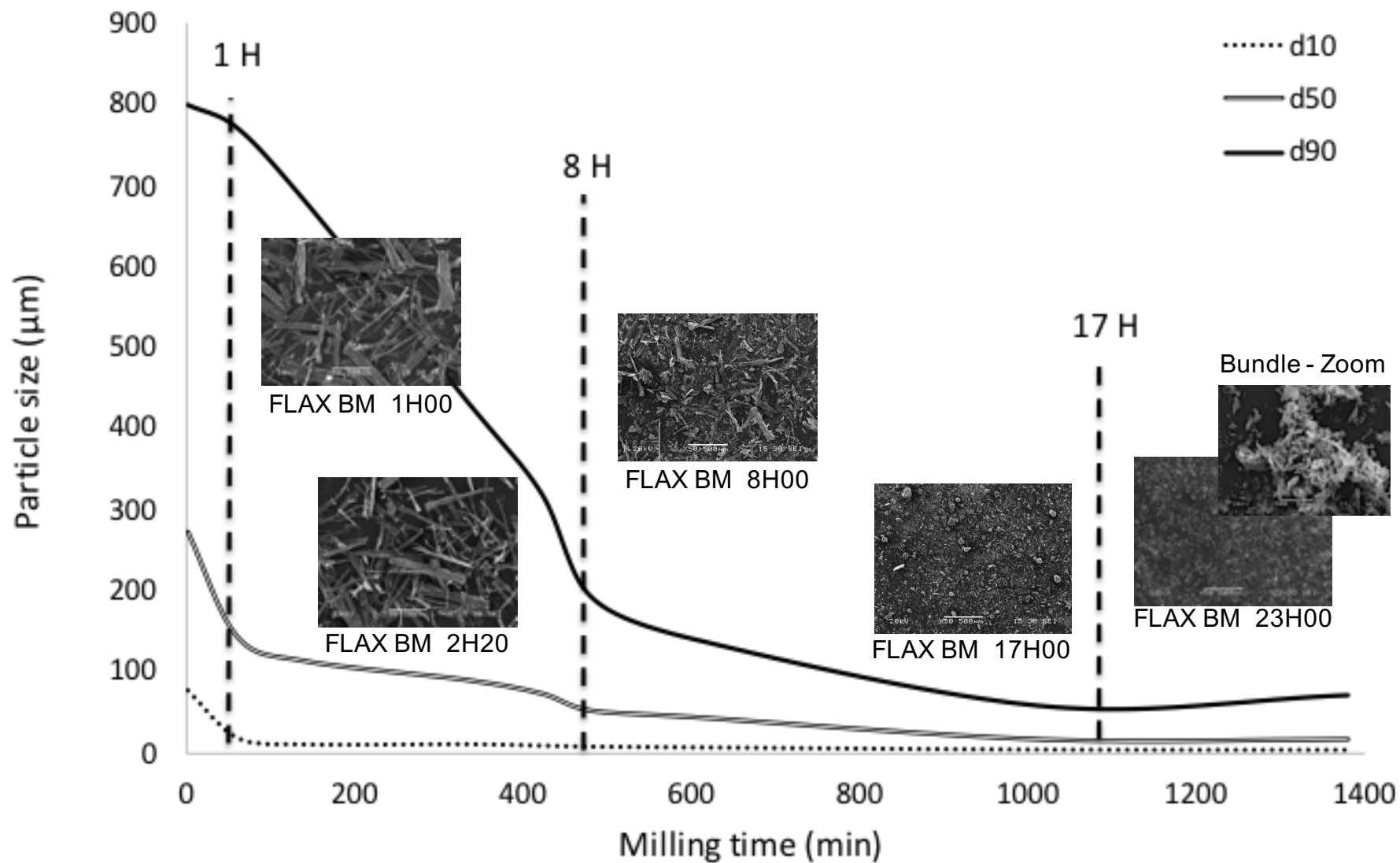
$L_w = 380 \mu\text{m}$   
 $D_w = 31 \mu\text{m}$   
 $L_w/D_w = 12$

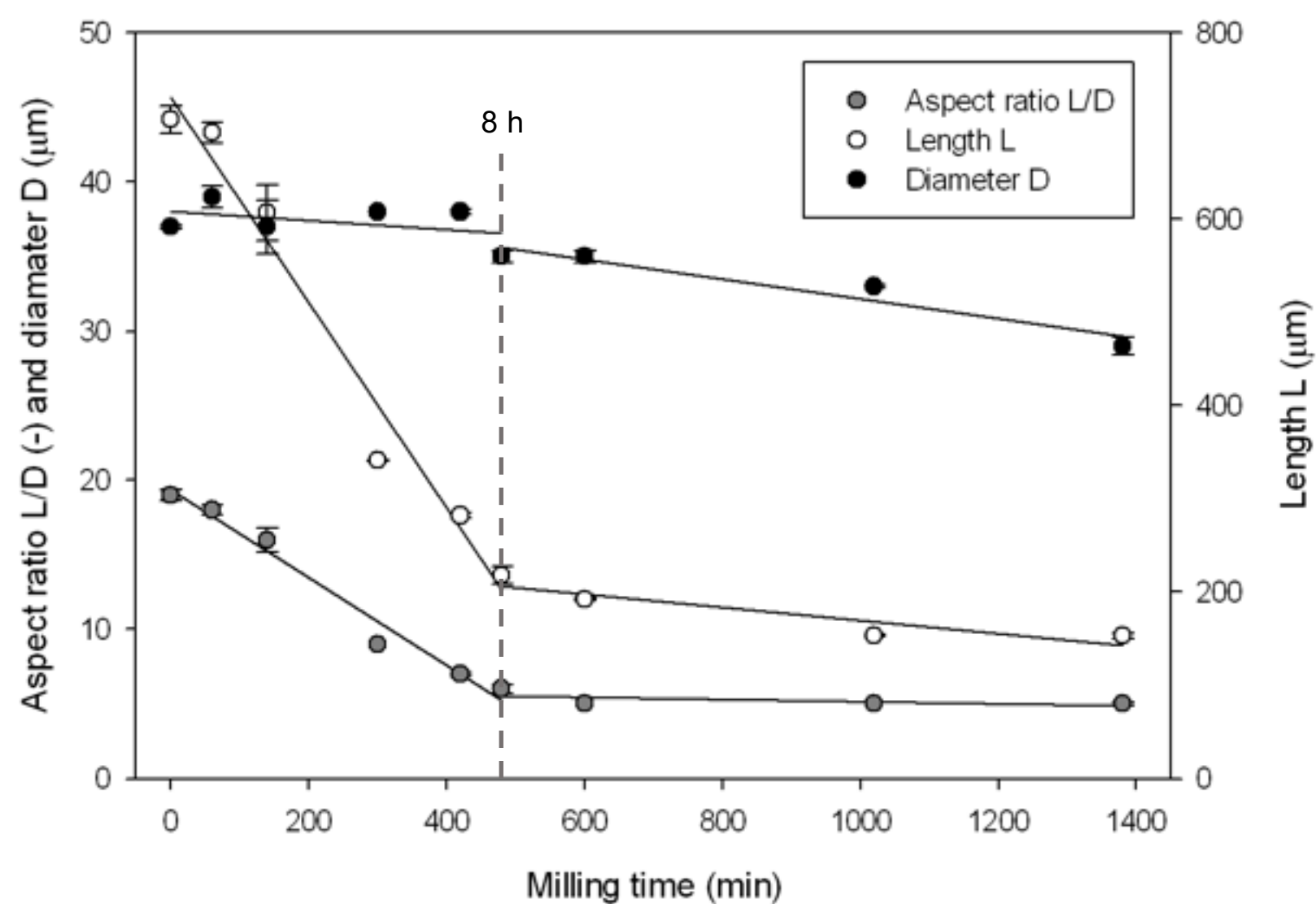


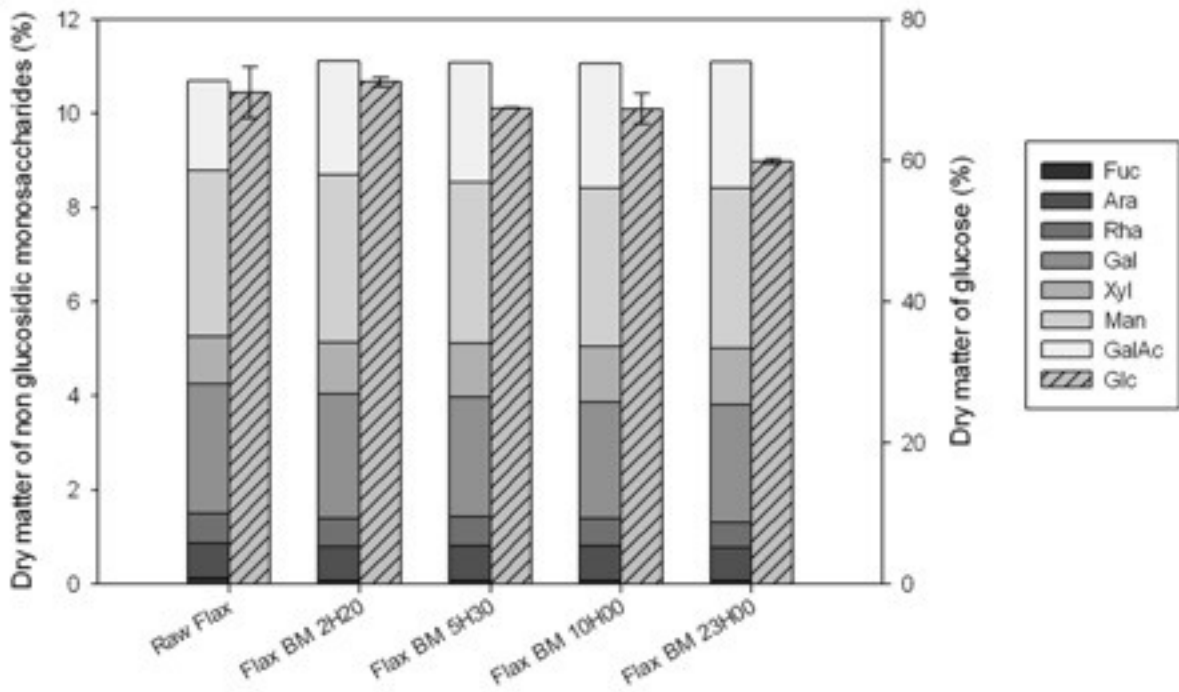
**FLAX 4**

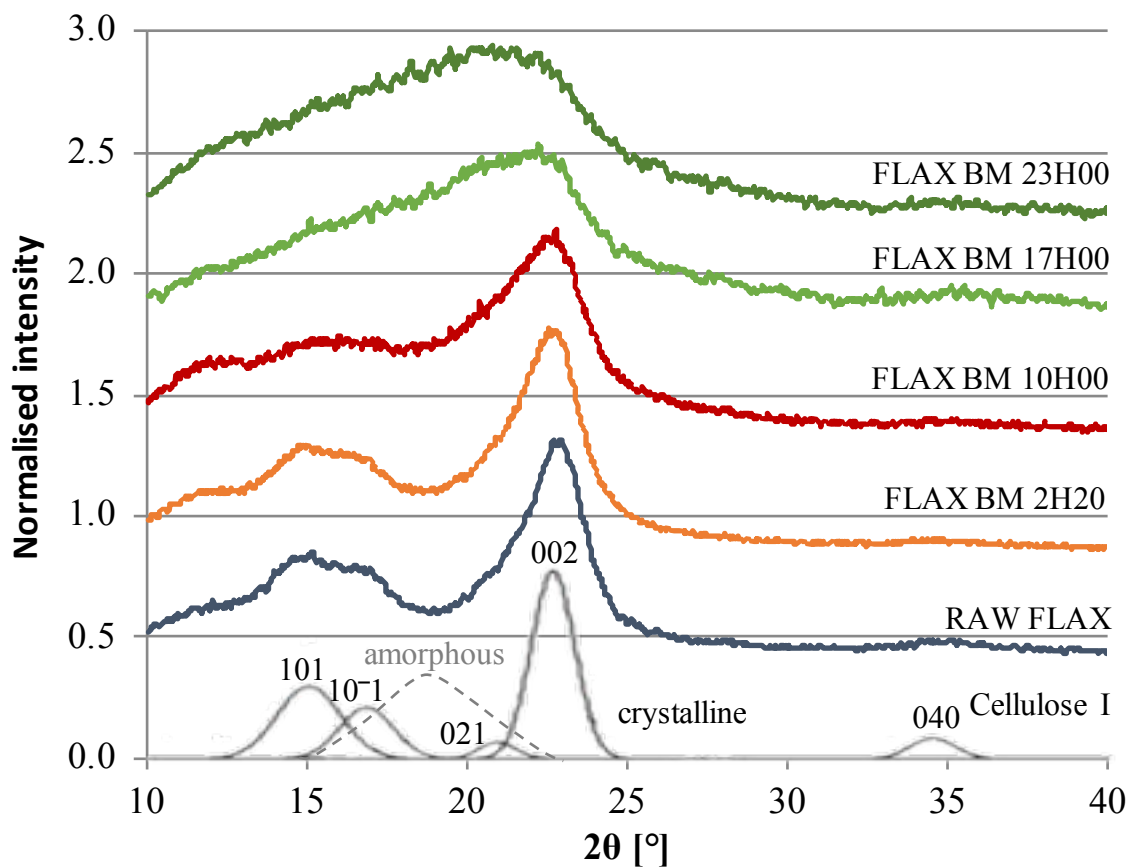
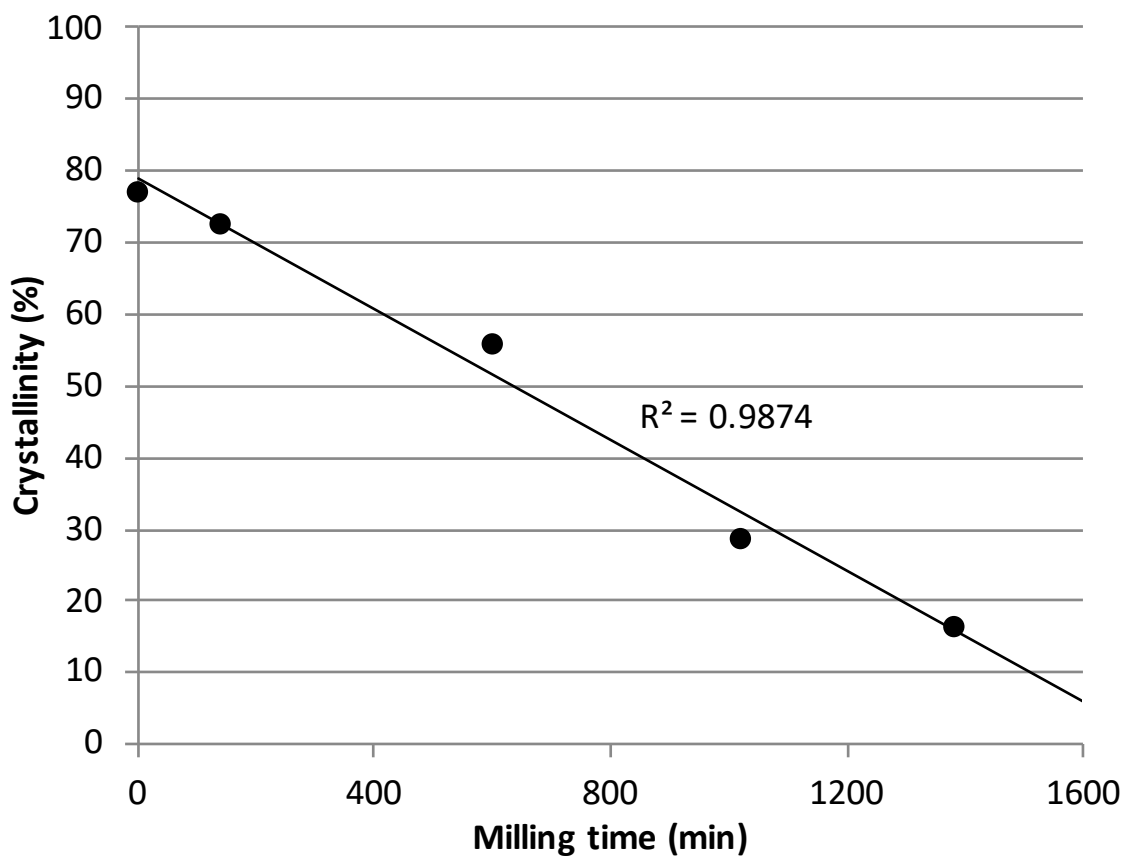
$L_w = 262 \mu\text{m}$   
 $D_w = 29 \mu\text{m}$   
 $L_w/D_w = 9$

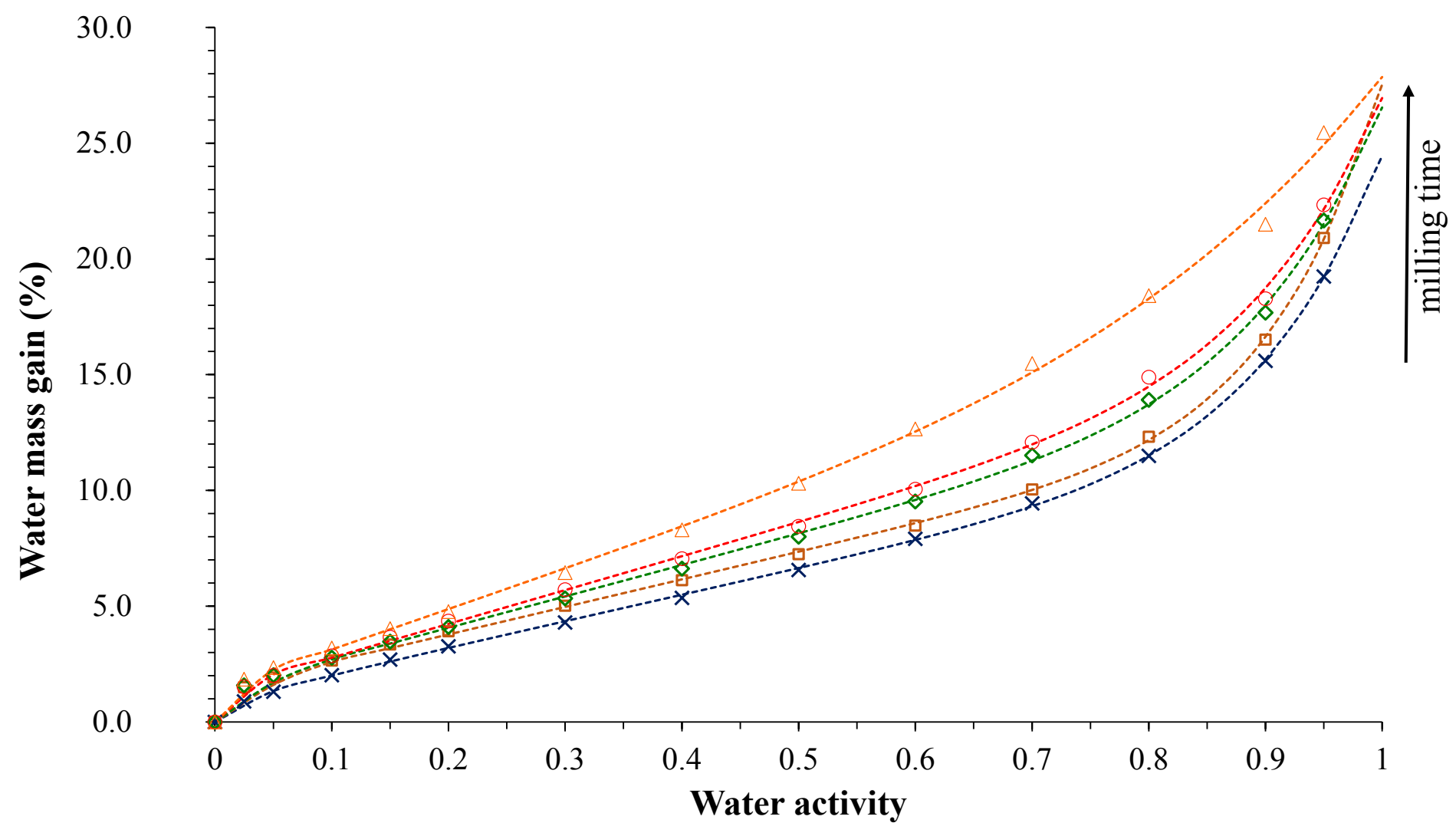








**a****b**



× RAW FLAX

□ FLAX BM 2H20

◇ FLAX BM 5H30

○ FLAX BM 10H00

△ FLAX BM 17H00

—●— RAW FLAX

—●— FLAX BM 10H00

—●— FLAX BM 23H00

Normalised  
crystallinity

1  
0,9  
0,8  
0,7  
0,6  
0,5  
0,4  
0,3  
0,2  
0,1  
0

Normalised milling  
energy

Normalised fibre  
length

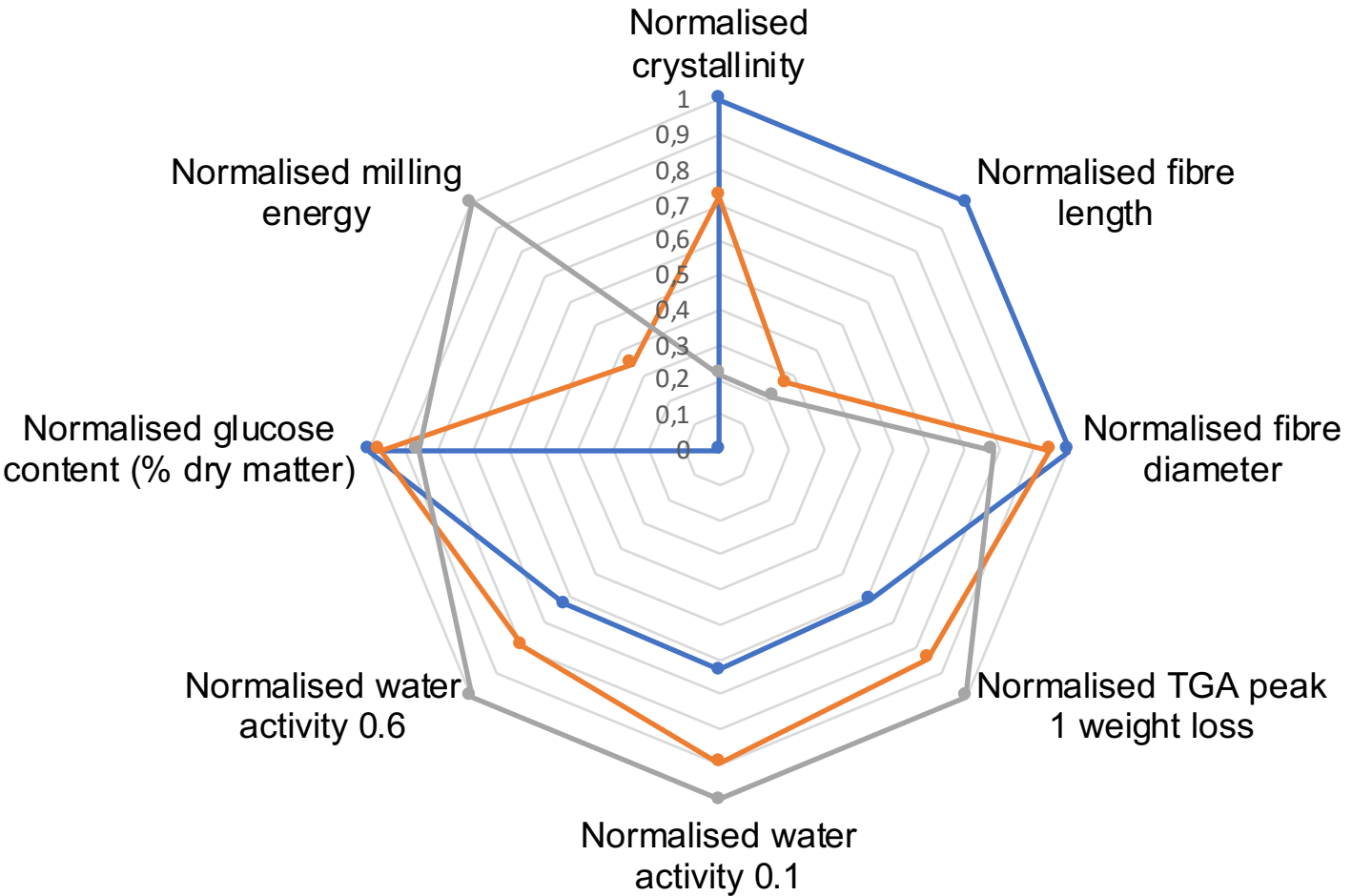
Normalised glucose  
content (% dry matter)

Normalised fibre  
diameter

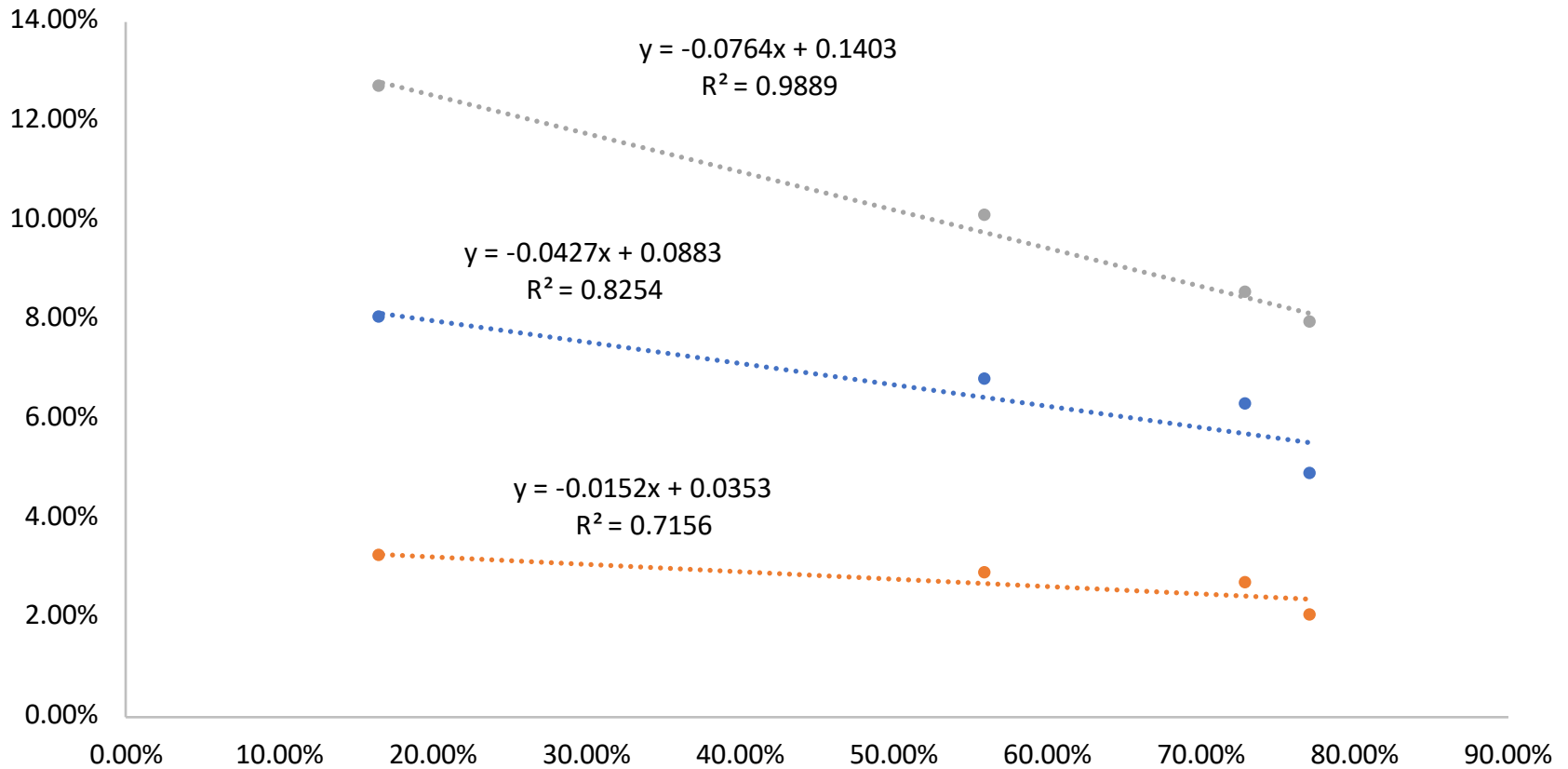
Normalised water  
activity 0.6

Normalised TGA peak  
1 weight loss

Normalised water  
activity 0.1



# Sorbed water content vs cristallinity



● Weight Loss (%) (1 peak in TGA)

● Water activity at 0.1 (%)

● Water activity at 0.6 (%)

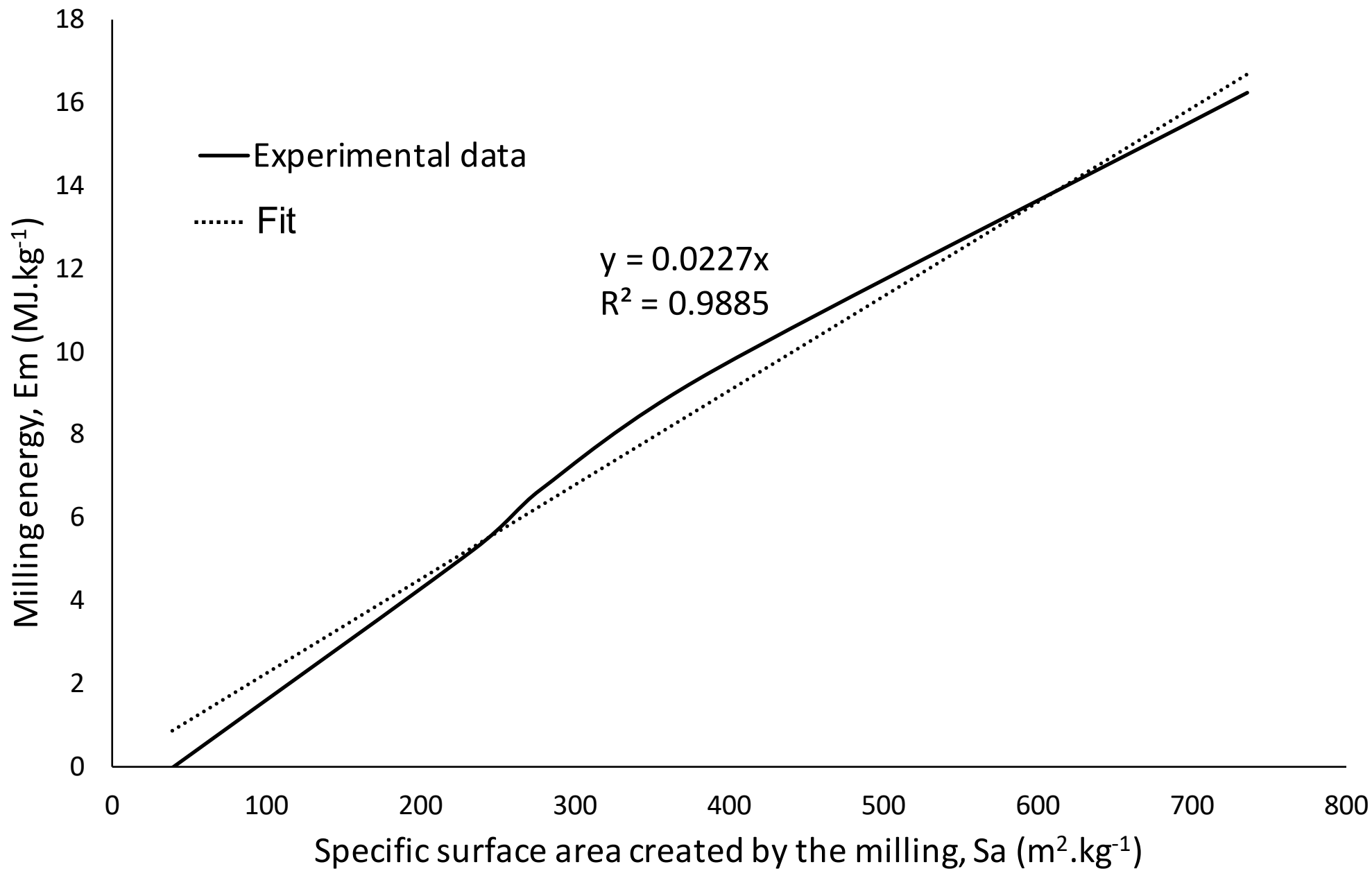


**Table 1.** Thermo-gravimetric analysis on flax fibres and fines. Temperatures are indicated for inflection points of weight loss curves.

| <i>Materials</i> | <i>First peak</i>      |                         | <i>Second peak</i>     |                         | <i>Third peak</i>      |                         |
|------------------|------------------------|-------------------------|------------------------|-------------------------|------------------------|-------------------------|
|                  | <i>Weight loss (%)</i> | <i>Temperature (°C)</i> | <i>Weight loss (%)</i> | <i>Temperature (°C)</i> | <i>Weight loss (%)</i> | <i>Temperature (°C)</i> |
| RAW FLAX         | 4.84                   | 60.9                    | 63.7                   | 320                     | 29.9                   | 402                     |
| FLAX BM 2H20     | 6.25                   | 56.8                    | 70.0                   | 314                     | 22.3                   | 421                     |
| FLAX BM 5H30     | 6.17                   | 58.2                    | 70.1                   | 307                     | 21.5                   | 407                     |
| FLAX BM 10H00    | 6.74                   | 59.7                    | 70.3                   | 298                     | 20.9                   | 394                     |
| FLAX BM 17H00    | 7.21                   | 65.2                    | 69.5                   | 292                     | 20.8                   | 383                     |
| FLAX BM 23H00    | 7.98                   | 67.8                    | 68.5                   | 284                     | 20.9                   | 366                     |

Table 2. Parameters of the Park model for the raw fibre and the treated fibres as a function of duration of ball milling.

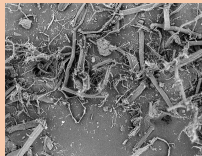
| Samples       | $A_L$ | $b_L$ | $K_H$ | $K_a$ | $n$ | $R^2$ | MRD (%) |
|---------------|-------|-------|-------|-------|-----|-------|---------|
| RAW FLAX      | 1.01  | 63.6  | 11.3  | 12.1  | 9   | 0.999 | 1.3     |
| FLAX BM 2H20  | 1.66  | 38.3  | 11.5  | 14.3  | 11  | 0.999 | 4.8     |
| FLAX BM 5H30  | 1.59  | 43.8  | 13.2  | 11.7  | 9   | 0.999 | 4.8     |
| FLAX BM 10H00 | 1.31  | 38.9  | 14.6  | 11.0  | 9   | 0.999 | 2.6     |
| FLAX BM 17H00 | 2.22  | 24.1  | 15.5  | 10.1  | 4   | 0.999 | 5.5     |



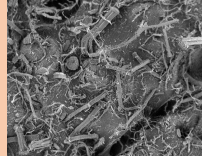
RAW FLAX - 1mm



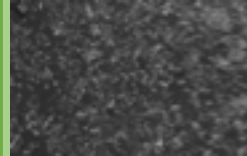
Impact Mill



Shear Mill

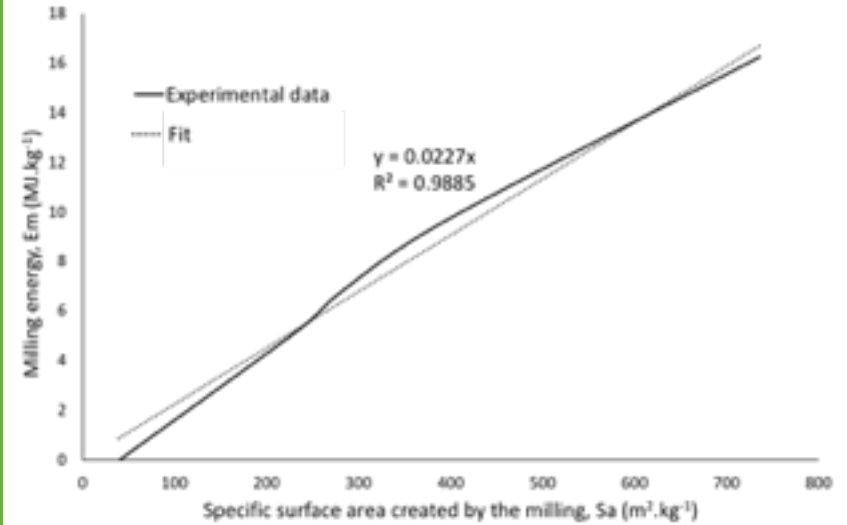


Ball Mill



Different  
milling times  
=> 1400  
min

Thinly influence on the size and  
on the morphology of the  
particles.



Strong influence on the physical and chemical  
characteristics of flax fibres.

